KINETICS OF DISCONTINUOUS PRECIPITATION AND COARSENING IN Ni - In ALLOY

A Thesis Submitted
in Partial Fulfilment of the Requirements
for the Degree of

MASTER OF TECHNOLOGY

by

SHATENDRA SINGH

to the

DEPARTMENT OF METALLURGICAL ENGINEERING
INDIAN INSTITUTE OF TECHNOLOGY, KANPUR

JULY, 1990

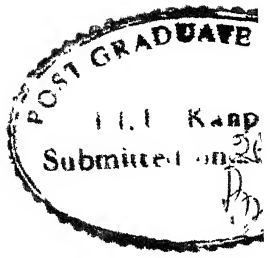

CERTIFICATE

This is to certify that the thesis entitled *"Kinetics of Discontinuous Precipitation and Coarsening in Ni-In Alloy"* is a bonafide record of work done by *"SHATENDRA SINGH"* in partial fulfilment of the requirements of M. Tech degree, under my supervision and has not been submitted elsewhere for the award of a degree.

July, 1990

(Dr. S P Gupta)

Professor

Department of Metallurgical Engineering

Indian Institute of Technology

Kanpur-208016.

ACKNOWLEDGEMENTS

I am indebted to my thesis supervisor Professor S P. Gupta for suggesting an interesting and amenable problem. I thank him for his valuable guidance and encouragement throughout the work

My special thanks goes to Mr K P. Mukherjee for his timely help. I am grateful to all my friends for the help extended to me during my stay at I.I.T.Kanpur.

Shatendra Singh

CONTENTS

LIST OF FIGURES

LIST OF TABLES

ABSTRACT

The morphology and growth kinetics of cellular precipitate and discontinuous coarsening have been studied in the temperature range 740 - 1010 K The Ni-In alloy was found to decompose completely by cellular precipitation reaction into lamellar structure consisting of α and θ phases at all the aging temperatures. The fine lamellar structure of the primary cells transformed into a coarse lamellar structure consisting of same two phases by a discontinuous coarsening reaction. Lattice parameter measurements indicated that depleted matrix was richer in solute than the equilibrium solvus composition during the primary reaction but it was very close to equilibrium solvus during the secondary reaction.

The primary cell growth data were analysed by using theories of Cahn, Hillert, Turnbull, Sundquist and Petermann and Hornbogen. The secondary cell growth data were analysed using theories of Livingston and Cahn and Petermann and Hornbogen. The driving force for the transformation was calculated from the regular solution model. The analysis indicated that the transformations are controlled by diffusion of In through the migrating grain boundaries.

Chapter 1. INTRODUCTION

Supersaturated Nickel rich Nickel-Indium alloys containing from 1.4 to 8 at% In have been observed to decompose completely by discontinuous precipitation during aging into a lamellar mixer of face centered cubic (fcc) nickel depleted α solid solution and θ (Ni_3In of DO_{19} structure) precipitate [1-4]. In these alloys a discontinuous coarsening reaction has also been observed to convert a fine lamellar structure produced by discontinuous precipitation into the coarser one [1,4,5]. The kinetics aspects of the primary and secondary cellular reactions have been studied in alloys containing Ni -2 at % In [6], Ni - 7·5 at % In [7], and Ni - 8 at % In [8], by optical microscopy and scanning electron microscopy It is shown that discontinuous precipitation and coarsening are controlled by grain boundary diffusion along the reaction front [6,7,8]. In the present investigation the morphology and growth kinetics of precipitation and coarsening of the cellular precipitate has been studied in a Ni - 4 at % In alloy, the objective being to determine diffusivity values and establish the rate controlling process

1·1 Preview of the work

The full thesis has been divided into five chapters All the theories which have been proposed for primary and secondary reactions [9-14] explanation, have been discussed in short in the first chapter.

The second chapter contains the experimental procedures of the present study which have been carried out for Ni - 4 at % In alloy

The third chapter deals with the kinetics aspects of the primary and secondary reactions. It presents the results along with a detailed discussion,

obtained through analysis of the primary reaction using the theories of Cahn [9], Turnbull [10], Hillert [11], Sundquist [12], Petermann and Hornbogen [13], and of the secondary reaction using model proposed by Livingston and Cahn [20] and Petermann and Hornbogen [13].

The conclusions drawn from the results obtained, are listed in the fifth chapter.

1·2 Discontinuous precipitation

The supersaturated solid solution dissociates at lower temperatures into solute depleted phase and solute rich phase (precipitate) as a duplex usually lamellar transformation behind a grain boundary advancing into a supersaturated matrix has been termed as **the discontinuous precipitation , cellular precipitation, grain boundary reaction** etc The precipitation is called discontinuous because only those regions are transformed which are being swept by the migrating grain boundaries. In majority of the alloy systems undergoing cellular precipitation, the growth kinetics show that for a given temperature and alloy composition in the absence of other precipitation reaction, rate of advance of cellular interface is constant and the same is cotrolled by rate of diffusion of solute in the advancing interface.

The cellular morphology which developes during transformation is dependent on the initiation of the solute rich phase (precipitation) and its subsequent growth in the form of a cell. The detailed study has been done over the initiation of this type of reaction. For discontinuous precipitation to occur

(i) An early suggestion was that a minimum precipitation / matrix misfit parameter $\delta = \frac{a - a_0}{a_0}$ of 1% is necessary for the reaction to occur Although this is based primarily on the strain energy criterion, a number of alloy systems with a value of δ less than 1% decompose into lamellar product by the cellular transformation.

(ii) According to Bohn [14], for Cu-base alloys cellular reaction would occur if the difference in solvent/solute atomic diameters is more than 11%. Exception to this proposal is the Cu-Cd alloy which undergoes cellular transformation.

(iii) Meyrick [15] proposal tried to quantify the occurrence of the cellular reaction and is based upon the change in the grain boundary energy with solute segregation. He considered a circular segment of the grain boundary pinned at points a distance '2r' apart, bulging forward by a distance 'x' Accordingly, for cellular reaction to occur

$$-\frac{\partial \gamma_{gb}}{\partial X_B} \geq \frac{2 \times \gamma}{\left({}^{i}X_B^{\alpha} - X_B^{\alpha} \right) r^2} \qquad (1.1)$$

where

$\frac{\partial \gamma_{gb}}{\partial X_B}$ = rate of change of grain boundary energy with increase in solute segregation at the boundary.

${}^{i}X_B^{\alpha}$ = original alloy composition

X_B^{α} = depleted matrix composition

Driving force to move a segment of the grain boundary, comes from the release of the energy due to decrease in the grain boundary energy because of solute segregation. If the release of the energy is high from the increase in the grain boundary energy due to grain boundary precipitation then it can induce the boundary to migrate in search of fresh solute . The inequality (1.1) examines whether enough solute content is present in the boundary to be energetically favourable for initial movement of the reaction front. Because of inaccuracy in the measurement of grain boundary energy with solute content, elements of uncertainty results, in the inequality of equation (1·1)

With majority of alloys undergoing cellular transformation, it has been well established that the nucleation of solute rich precipitate takes place on the grain

boundary and the reaction occurs from the high mobility of the boundary. It is common observation that fraction of the grain boundaries do not transform or transform very late. This is because of the grain boundary structure and its orientation. According to Smith [16] grain boundaries with misorientation of more than 11° undergo cellular transformation predominantly.

In brief, it can be stated that none of the concepts mentioned above are applicable to all alloy systems and there are allways some alloy system which show exception but nonetheless undergo cellular reaction.

1.3 Initiation of cellular reaction

The occurrence of heterogeneous nucleation of grain boundary precipitate and the ability of the grain boundary to migrate, is directly related to the initiation of the discontinuous reaction. Thus the mechanisms of the cellular reaction can be classified into two categories

1. Precipitation induced grain boundary migration,
2. Boundary migration due to chemical potential difference across the cell boundary

The Tu and Turnbull 'Pucker' mechnism [17] for celllar transformation falls in the first category. Accordingly, the plate or disc shaped solute rich phase nucleates on the side of the grain boundary having high energy interface across the grain boundary and the habit plane with the grain in which it is embedded The specific interfacial energy of the habit plane is lower than the interface with the random orientation. A reduction in the interfacial energy of the precipitate can be achieved by migration of the grain boundary along the high energy interface,so as to embed the precipitate completely in the grain but attached to the boundary by its tip This reduction in the interfacial energy provides the initial driving force which results in local deflection of the grain boundary into a Puckered

configuration [19]. Now, one side of the grain boundary is favourably oriented to nucleate the second precipitate disc or plate. This process of grain boundary migration continues which builds up a series of parallel lamellae. As these parallel lamellae move forword, they carry the grain boundary along and the solute transfer occurs by boundary diffusion. Fig. 1·1 illustrates the above mechanism in Pb - Sn alloys.

Fournelle and Clark [18] proposed a mechanism for initiation of the cellular reaction which falls in the second category. It proposes that the grain boundaries migrate continuously from their low temperature configuration similar to that observed during grain growth. If the boundary precipitation occurs concurrently this is suffucient to stimulate the formation of cell nucleus. The migrating grain boundary gets pinned because of the formation of the allotriomorphs due to accumulation of solute on the boundary leaving behind a solute depleted region. The thermodynamic driving force develops due to chemical potential difference between the solute depleted region and matrix. Further migration of the grain boundary is favoured due to the thermodynamic driving force but only possible if it bows between the allotriomorphs The region behind the advancing grain boundary continues to be depleted of solute by its transfer across the boundary to the allotriomorphs which then begin to lengthen. This mechanism has been demonstrated step by step Fig.(1·2)

This mechanism does not require a regid habit and orientation relationship between the precipitate and matrix phases for cellular reaction in alloy system such as Fe-Zn and Cu-In etc, which show a lack of regid habit In the above mechanism a major discrepancy is in explanining the twisting of segments of a curved grain boundary in the form of an S

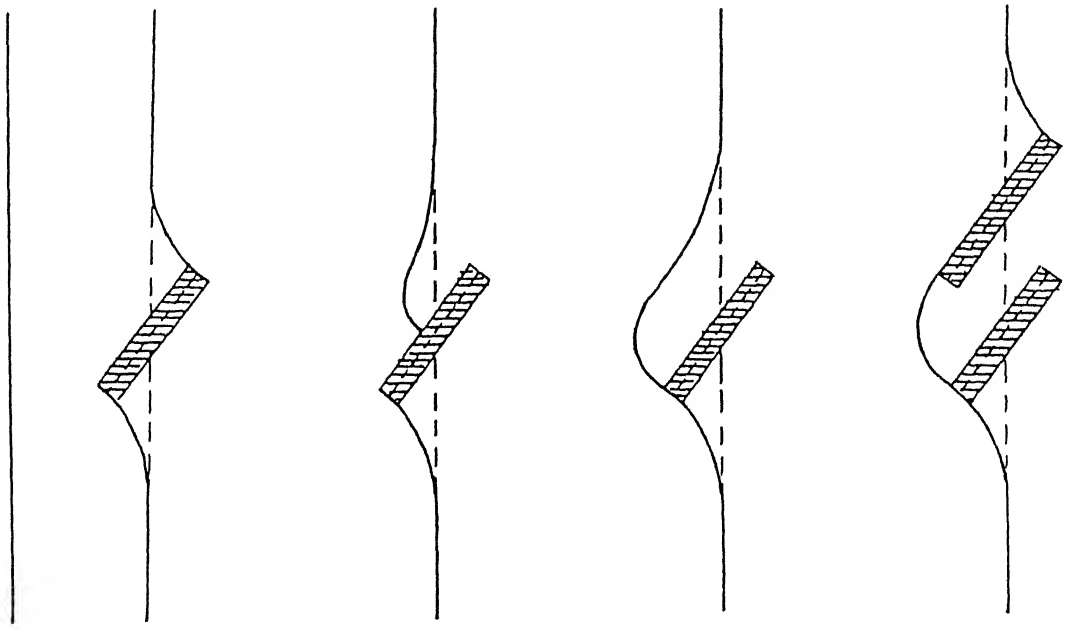

(a) Straight Interface

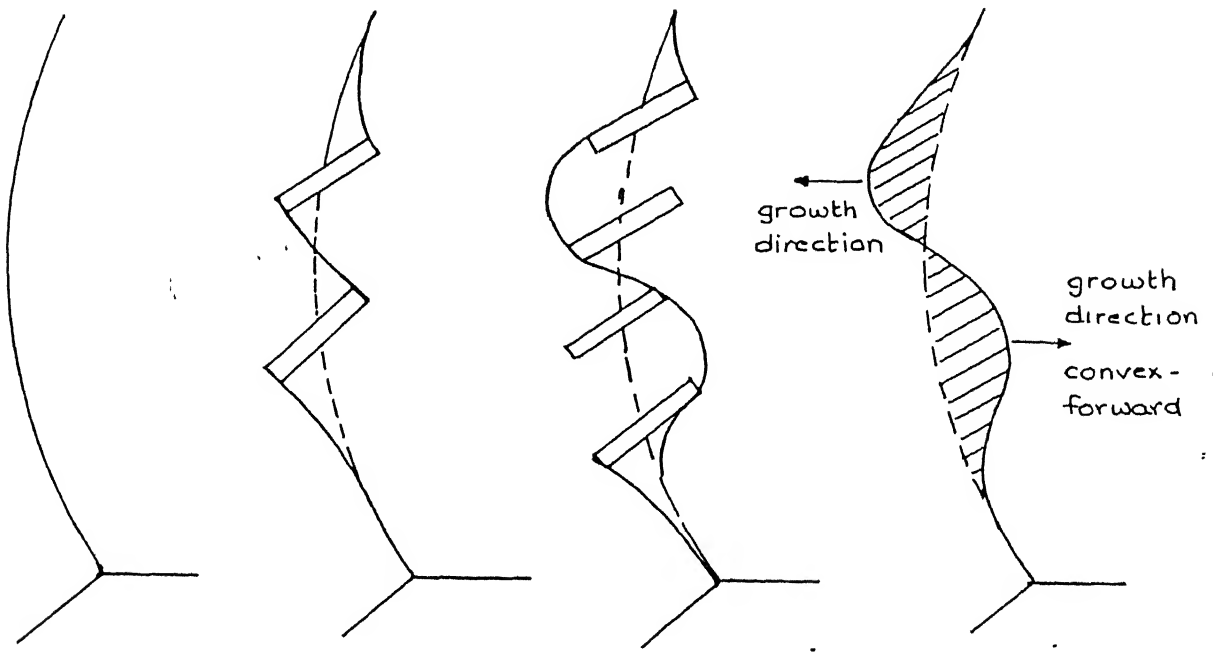

(b) Curved Interface

Fig. 1.1 Tu and Turnbull's Pucker Mechanism of cellular precipitation.

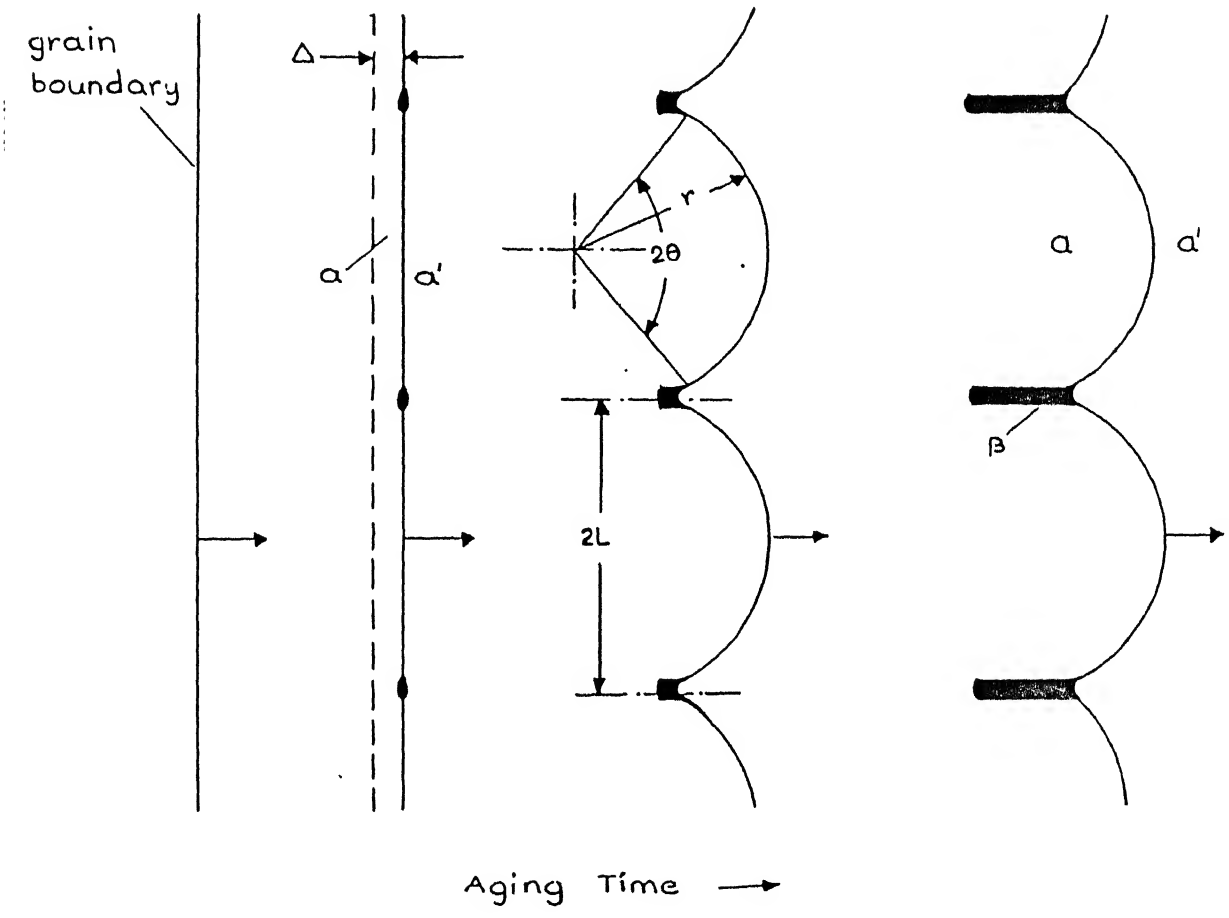

Fig. 1·2 Schematic diagram showing essential steps in nucleation of reaction on a migrating boundary; after Fournelle and Clark.

1·4 Growth of Discontinuous Precipitate

The growth of cell occurs basically by two mechanisms :

(i) growth of the cell primarily in one direction from the initial position

(ii) growth of the cell in both the directions

The one directional growth mechanism is proposed by Fournelle and Clark [18]. According to this mechanism the dominant factor for cell growth is migration of the grain boundary. Besides the few exceptions, this mechanism holds only in the range of temperatures where thermally activated migration of grain boundaries can occur

The mechanism of growth of cells in both the directions from an initially straight grain boundary is after Nes and Bildall [31] Accordingly, the grain boundary undergoes a convex - forward stance in either grain due to bulging of a straight grain boundary caused by nucleation of the precipitate The curvature of the advancing grain boundary determines the cell growth direction

During the growth of the discontinuous precipitate the lamellae multiplication occurs in a number of ways i e. branching, repeated nucleation and nucleation of lamellae in the recess.

1·5 Discontinuous coarsening

It has been determined that continued aging of the alloy decomposes the products of the primary cellular reaction into new products which consists of the same two phases but have larger interlamellar spacing Similar to the primary cell formation, decomposition occurs discontinuously and therfore it is known as discontinuons coarsening These secondary cells nucleate either on one side or both sides of the grain boundaries in adjacent region, in a similar manner as with the primary cells. The secondary cells nucleate

(i) at prior grain boundary by the 'S' - mechanism

(ii) at the intersection of two primary cells

(iii) at the intersection of primary cells with the grain boundary

In the S-mechanism proposed by Fournelle [19], adjacent segment of a grain boundary between two grains are observed to advance into opposite grains leaving behind cellular lamellae with greater spacing, oriented with respect to the grain from which they originated, Fig 1·3. If the growth continues they pivot about a common point on the original grain boundary in such a way that migrating boundary of both cells grow into the origin of its counterparts at the original position of the grain boundary.

The other mechanism proposes that the secondary cells nucleate and grow from impinged regions of the primary cells which can lead to growth in one or both directions from the common cell boundary.

1·6 Driving Force For Discontinuous Precipitation

The following driving force can be taken into consideration depending upon the mechanism which operates to nucleate the precipitate, for the initiation of the cellular phase transformation.

$$\Delta G = \Delta G_{ppt} + \Delta G_{\varepsilon} + \Delta G_{gb} \qquad (1.2)$$

where the thermodynamic driving force ΔG_{ppt} arises from the chemical driving force due to difference in the solute content between the super saturated solid solution and the depleted matrix. Due to super saturation at the aging temperature initial precipitate nucleates. After the nucleation, a small but finite amount of energy is released if both the interfaces of the precipitate have low energy interface and are embedded in the same grain of the solute depleted region. This finite amount of energy released is consumed to deflect the boundary into an

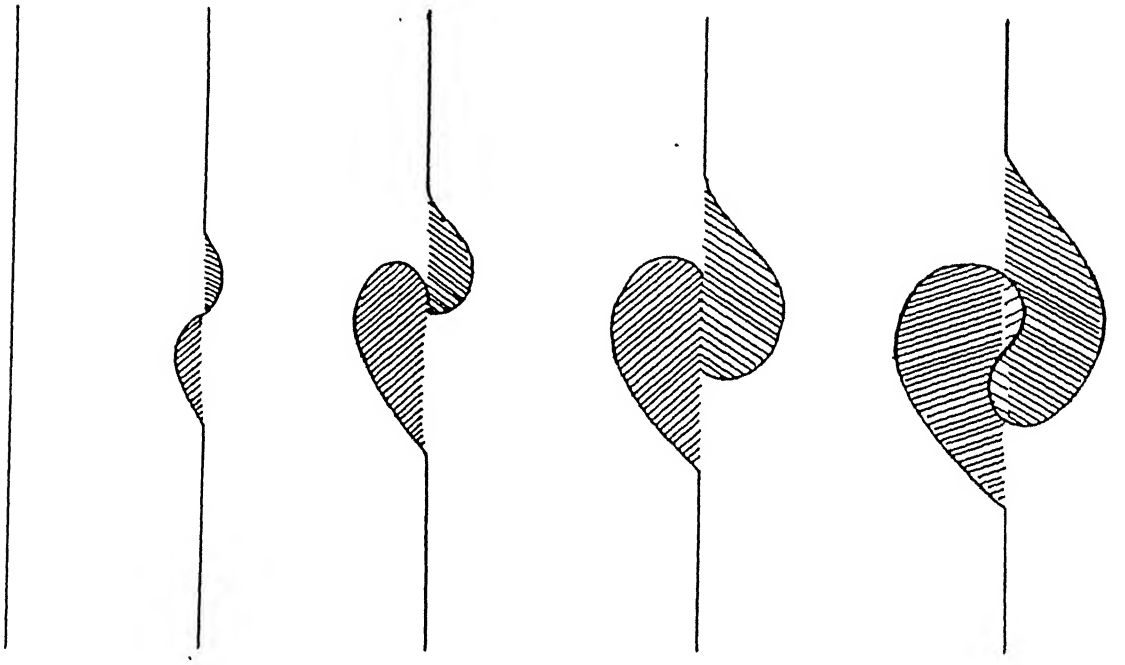

Fig. 1.3 Fournelle's 'S' mechanism schematic illustration.

equilibrium position locally The mechanism proposed by Nes and Bildal [31] exhibits that the chemical free energy is used as a driving force for the nucleaton of the precipitate and the boundary moves under the chemical potential difference across the boundary but gets pinned at the precipitate Further migration is possible under chemical driving force for the primary cellular precipitation

In the mechanism of Fournelle and Clark [18] the initial migration of the boundary occurs under the driving force of the chemical potential difference across the boundary in order to obtain stable low energy configuration. As the boundary advances, it deposits solute resulting into nucleation of the precipitate The boundary continues its migration under the chemical driving force for the discontinuous precipitation As the grain boundary sweeps through the super saturated matrix, the solute diffusion across it transfers more solute to the growing precipitate. If the diameter of the solute atom is significantly different from that of the solvent atom, strain are set up in the vicinity of the boundary. Thus, a part of the available chemical driving force is used in the form of strain energy ΔG_{ε}.

The available chemical free energy ΔG_1 calculated at the original alloy composition is divided into separate parts as follows

$$\Delta G_0 = \Delta G_1^{C} + \Delta G_1^{\gamma} \left(\frac{2 \gamma V_m}{S_1} \right) + \Delta G^{C}_2 \qquad (1.3)$$

where

ΔG_0 = total chemical driving force

ΔG_1^{C} = the chemical free energy available for the primary cell growth and is equal to $P\Delta G_0$ used by Cahn where P is fraction of ΔG_0

ΔG_2^{C} = Chemical driving force retained in the matrix of the primary cells

ΔG_i^{γ} = Reversible surface energy associated with α/θ interface

Cahn pointed out if the rate of migration of the cell boundary is finite, then the solute partitioning is not complete which results in higher average concentration in the depleted phase after completion of the primary reaction. Thus, a part of the available chemical force is retained in the matrix of the primary cells. During discontinuous coarsening, a part of the surface energy associated with primary cells is also used. In this sense, the surface free energy ΔG_i^{γ} is reversible

1·7 Kinetics of Cellular Phase Transformation

1·7·1 Turnbull 's Model for Growth Kinetics [10]

Let us consider the precipitation of θ-phase morphology, a super saturated solid solution α_0 forming a lamellar morphology. According to Zener's treatment [32] of pearlitic transformation total flow away from a lamella can be determined from Fick 's first law $J = -\Delta\frac{dc}{dx}$ to give the rate of flow of atoms

$$\frac{dm}{dt} = \frac{A^{\alpha}D}{V_m}, \quad \frac{dX_B}{dx} = \frac{A^{\alpha}D}{V_m}\frac{X_B}{L_{eff}} \tag{1.4}$$

A^{α} = Area through which the diffusion takes place

D = Diffusion coefficient of the solute in the matrix

$\frac{X_B}{L_{eff}}$ = Concentration gradient (Left - effective diffusion distance)

V_m = molar volume

This model is based upon diffusion of the solute through the grain boundary. In equation (1·4), the value of A^{α} will be $b\delta$, where δ is the grain boundary thickness and b is the distance parameter perpendicular to the growth direction and α/θ interface. The effective diffusion length has been investigated to be equal to S^{α} which upon substitution in equation (1·4) yields

$$\frac{dm}{dt} = \frac{b\ \delta\ D_b}{V_m}\ \frac{\Delta X_B}{S^{\alpha}} \qquad (1.5)$$

During primary cell transformation, α and θ phases grow together as alternate lamellae. The width of the lamallae is related by lever rule as

$$\frac{S^{\alpha}}{V_m} = \frac{X_B^{\theta} - {}^{i}X_B^{\alpha}}{X_B^{\theta} - X_B^{\alpha}}\ \frac{S}{V_m} \quad \text{and} \quad \frac{S^{\theta}}{V_m} = \frac{{}^{i}X_B^{\theta} - X_B^{\alpha}}{X_B^{\theta} - X_B^{\alpha}}\ \frac{S}{V_m} \qquad (1.6)$$

which gives

$$\frac{dm}{dt} = V\ b\ \frac{S^{\alpha}}{V_m}\ (\ {}^{i}X_B^{\alpha} - X_B^{\alpha}\ ) = V\ b\ \frac{S^{\theta}}{V_m}\ (\ X_B^{\theta} - {}^{i}X_B^{\alpha}\ )$$

$$= V\ b\ \frac{S}{V_m}\ f^{\alpha}\ f^{\theta}\ (\ X_B^{\theta} - X_B^{\alpha}\ ) \qquad (1.7)$$

Equating (1·7) and (1·5)

$$V\ b\ \frac{S^{\alpha}}{V_m}\ (\ {}^{i}X_B^{\alpha} - X_B^{\alpha}\ ) = \frac{D_b\delta}{V_m}\ \frac{\Delta X_B}{S^{\alpha}}$$

$$V = \frac{D_b\ \delta}{(\ {}^{i}X_B^{\alpha} - X_B^{\alpha}\ )}\ \frac{\Delta X_B}{(S^{\alpha})^2} \qquad (1.8)$$

In approximating ΔX_B , which drives the diffusion. Turnbull [10] neglected the effect of surface energy and used $\Delta X_B = {}^{i}X_B^{\alpha} - X_B^{\alpha/\theta}$ In addition he neglected X_B^{α} in comparison to ${}^{i}X_B^{\alpha}$,the original alloy composition and thus , came out with the following expression for growth velocity

$$V = \frac{D_b\ \delta}{(S^{\alpha})^2}\ \frac{{}^{i}X_B^{\alpha} - X_B^{\alpha/\theta}}{{}^{i}X_B^{\alpha}} \qquad (1.9)$$

1·7·2 Cahn Treatment Of Discontinuous Precipitation [9]

It has been suggested by Cahn [9] that α lamallae in equilibrium with θ is not equilibrium composition. Due to incomplete segregation of solute only a fraction of the total free energy available will be used to drive the reaction The remaining $\left(\frac{2\gamma V_m}{S} \right)$ will be assssociated with the newly formed interface. It is further assumed that the reaction proceeds as far as diffusion permits and the interface is flat and no diffusion occurs except at the boundary Under steady state conditions,

$$\frac{dX_B^{\alpha}}{dt} = \frac{D_{b\delta}}{V_m} \frac{d^2 {}^{b}X_B^{\alpha}}{dy^2} + \frac{V}{V_m} \left({}^{i}X_B^{\alpha} - X_B^{\alpha} \right) = 0 \qquad (1.10)$$

where

V = growth velocity

${}^{b}X_B^{\alpha}$ = concentration of solute at the boundary

${}^{i}X_B^{\alpha}$ = original alloy composition

X_B^{α} = cncentration of the solute in the deblated matrix

y = distance along the boundary measured perpendicular to the lamallae

Assuming X_B^{α} to be proportional to ${}^{b}X_B^{\alpha}$ with a proportionality constant K the equation (1·10) can be solved. Cahn also assumed that $\left(X_B^{\alpha} / {}^{b}X_B^{\alpha} \right)$ = K constant . Equilibrium prevails at the interface and that θ lamallae are thin with respect to the interlamellar spacing. Thus, the boundary conditions are

$$X_B^{\alpha} = e\, X_B^{\alpha} \quad \text{at} \quad Y = \pm \frac{S}{2}$$

The equation (1·10) solution is given by

$$\frac{X_B^{\alpha} - {}^{i}X_B^{\alpha}}{{}^{e}X_B^{\alpha} - {}^{i}X_B^{\alpha}} = \frac{\cosh\left(\frac{Y}{S}\sqrt{A}\right)}{\cosh\left(\frac{1}{2}\sqrt{A}\right)} \qquad (1.11)$$

where

$$A = \left(\frac{K\ V\ S^2}{D_b\ \delta}\right)$$

Cahn [9] approximated the chemical free energy for non equilibrium segregation as

$$\Delta G_c = -RT\left({}^{i}X_B^{\alpha} \ln \frac{{}^{i}X_B^{\alpha}}{{}^{e}X_B^{\alpha}} + {}^{i}X_B^{\alpha} \ln \frac{{}^{i}X_A^{\alpha}}{{}^{e}X_A^{\alpha}}\right)\left(1 - \frac{X_B^{\alpha} - {}^{e}X_B^{\alpha}}{{}^{i}X_B^{\alpha} - {}^{e}X_B^{\alpha}}\right)$$

According to Cahn's treatment the fraction of solute used during cellular reaction precipitation can be evaluated as

$$W = \frac{2}{\sqrt{A}} \tanh \frac{\sqrt{A}}{2} \qquad (1.12)$$

where $W = \dfrac{{}^{i}X_B^{\alpha} - X_B^{\alpha}}{{}^{i}X_B^{\alpha} - {}^{e}X_B^{\alpha}}$

Thus, value of A can be calculated.

1·7·3 Peterman And Hornbogen 's Treatment [13]

Accordingly, the growth velocity is given by

$$V = -M\ \Delta G_1 \qquad (1.13)$$

where M = grain boundary mobility

ΔG_1 = available driving force for the growth of the primary cells

The mobility is a function of temperature and determined by the atomic jump

frequency τ^{-1} and the grain boundary thickness δ, for growth of the phases and simultaneous migration of the grain boundary Solute atoms existing at the grain boundary must diffuse a distance $\frac{S}{2}$ to the θ lamellae. The time for atoms to move a distance $\frac{S}{2}$ is

$$\frac{S^2}{4} = 2\, D_b\, \tau \qquad \Rightarrow \qquad \tau = \frac{S^2}{8\, D_b}$$

which gives

$$V = - \frac{8\, D_b\, \delta}{RT\, S^2}\, \Delta G_1 \tag{1.14}$$

With the help of free energy composition diagram, the amount of chemical free energy available to drive the reaction can be evaluated

$$\Delta G = P \Delta G_0 + \frac{2\gamma\, V_m}{S} \tag{1.15}$$

where γ = specific surface energy of α/θ interface

P = fraction of the chemical free energy ΔG_0 released during the reaction,

$$\text{or,} \quad \Delta G = RT \left[{}^{1}X_B^{\alpha} \ln \left(\frac{X_B^{\alpha}}{{}^{1}X_B^{\alpha}} \right) + {}^{1}X_A^{\alpha} \ln \left(\frac{X_A^{\alpha}}{{}^{1}X_A^{\alpha}} \right) \right] + \frac{2\gamma\, V_m}{S} \tag{1.16}$$

The growth velocity equation is given by

$$V = - \frac{8\, D_b \delta}{S^2\, RT} \left\{ RT \left[{}^{1}X_B^{\alpha} \ln \left(\frac{X_B^{\alpha}}{{}^{1}X_B^{\alpha}} \right) + {}^{1}X_A^{\alpha} \ln \left(\frac{X_A^{\alpha}}{{}^{1}X_A^{\alpha}} \right) \right] + \frac{2\gamma\, V_m}{S} \right\} \tag{1.17}$$

1.7.4 Sundquist's analysis [12]

Sundquist [12] derived the diffusion equation on the lines of Cahn [9] but he worked out the diffusion equation for curved interface instead of assuming the flat interface between α_0 and θ as done by Cahn [9]. The basic solution of the differential equation gives

$$\frac{\bar{V}_{X_B}{}^{\alpha} - {}^{1}X_B{}^{\alpha}}{{}^{0}X_B{}^{\alpha} - {}^{1}X_B{}^{\alpha}} = \frac{\cosh\left(\sqrt{\alpha} - (1 - \bar{Y} \right)}{\cosh \sqrt{\alpha}} \qquad (1.18)$$

The parameter α is

$$\alpha = \frac{V_i \, S_i{}^2}{4 \, D_b \, \delta \, K \, (\overline{\cos \theta})} \qquad (1.19)$$

where $\bar{V}_{X_B}{}^{\alpha}$ = average composition of the depleted matrix at position ($\bar{Y}$) from the interface α and θ phases

${}^{0}X_B{}^{\alpha}$ = interface composition at the three phase junction

The value of ${}^{0}X_B{}^{\alpha/\theta}$ is very close to the equilibrium solvus composition ${}^{e}X_B{}^{\alpha/\theta}$ at the aging temperature but according to Sundquist [12], it is defined by

$${}^{0}X_B{}^{\alpha/\theta} = {}^{e}X_B{}^{\alpha/\theta} \exp\left[\frac{2 \, V_m \, \theta \, (X_B{}^{\theta} - X_B{}^{\alpha})}{RT \, S^{\alpha} \, ({}^{1}X_B{}^{\alpha} - {}^{e}X_B{}^{\alpha/\theta})} \right] \qquad (1.20)$$

where θ has a value of $\pi/6$.

$\overline{\cos \theta}$ is the average of the angle normal to the growth front direction and is taken to be 0.7 as proposed by Sundquist [12]. The fraction of the solute precipitate is given by

$$W = \left[\frac{{}^{i}X_B^{\alpha} - {}^{o}X_B^{\alpha/\theta}}{{}^{i}X_B^{\alpha} - {}^{e}X_B^{\alpha/\theta}} \right] \frac{\tanh \sqrt{\alpha}}{\sqrt{\alpha}} \qquad (1.21)$$

The parameter α is determined from the relation (1·21).

1.7.5 Hillert's Analysis [11]

According to Hillert's analysis [11], the Cahn's [9] treatment is based on the incorrect assumption that the composition of the matrix at the line of contact with precipitate β, at the growing cell front is equal to the equilibrium value ${}^{e}X_B^{\alpha}$ The composition of the three phase region can be obtained considering the driving forces for α and θ separately and assuming that the θ phase has constant composition which is as follows :

$$\frac{{}^{b}X_B^{\alpha} - {}^{o}X_B^{\alpha/\theta}}{{}^{i}X_B^{\alpha} - X_B^{\alpha}} = \frac{V_m (s^{\theta})^2}{8 D_b \delta} \left[1 - \left(\frac{2 Y}{S^{\theta}} \right)^2 \right] \qquad (1.22)$$

Applying the boundary diffusion control of Turnbull [10]

$$\frac{dm}{dt} = \frac{8 D_b \delta b K \Delta X}{V_m S}$$

to yield

$$V = \frac{8 K D_b \delta}{S . S^{\alpha}} \left[\frac{X_B^{\alpha} - {}^{o}X_B^{\alpha}}{{}^{i}X_B^{\alpha} - X_B^{\alpha}} \right] \qquad (1.23)$$

The compositions ${}^{o}X_B^{\alpha}$ and X_B^{α} are assumed constant although they are not. Hillert [11] has given explicit parameters thus enabling the diffusivity $KD_b\delta$ to be calculated from experimentally measured quantities.

1.7.6 Livingston and Cahn's Model for discontinuous coarsening

Livingston and Cahn [21] model proposes that the driving force for the discontinuous coarsening is the reduction in the free energy accompanying the formation of secondary cells with spacing S_2 from the primary cells with spacing S_1. Accordingly,

$$-\Delta G = 2\gamma V_m \left[\frac{1}{S_1} - \frac{1}{S_2} \right] \qquad (1\ 24)$$

Considering steady state, rate of the mass transport in front of the α lamella is

$$\frac{dm}{dt} = -D_b\ 2b\delta\ \frac{\Delta X_B}{(\ S_2{}^{\alpha}/2\ )} \qquad (1\ 25)$$

where $\Delta X_B = -\ {}^{b}X_B{}^{\alpha}\ \frac{2\gamma V_m}{RT\ S_1} \left[\frac{1}{S_1} - \frac{1}{S_2} \right]$ and

$\frac{S_2{}^{\alpha}}{2}$ = the effective diffusion distance using Zener's approximation

Again, rate of mass transport in front of the β lamella is given by

$$\frac{dm}{dt} = V_2\ b\ S_2{}^{\theta}\ (\ X_B{}^{\theta} - {}^{1}X_B{}^{\theta}\ ) \qquad (1\ 26)$$

Equation (1.25) and (1.26) yield,

$$V_2 = \frac{8\ KD_b\delta}{(\ f_2{}^{\alpha}\ )^2\ (\ f_2{}^{\theta}\ )} \left[\frac{{}^{0}X_B{}^{\alpha}}{X_B{}^{\theta} - X_B{}^{\alpha}} \right] \left[\frac{\gamma V_m}{RT\ S_1\ S_2{}^2} \right] \left[1 - \frac{S_1}{S_2} \right] \qquad (1\ 27)$$

where $K = \frac{{}^{b}X_B{}^{\alpha}}{{}^{0}X_B{}^{\alpha}}$

1.7.7 Petermann and Hornbogen's theory [13] of discontinuous coarsening

As shown earlier, the growth velocity of primary cells during discontinuous phase transformation is given by

$$V_1 = -\frac{8\, D_b \delta}{RT\, S_1^2}\, \Delta G_1$$

The subscript 1 denotes primary reaction. The chemical free energy ΔG_1 used to drive the reaction is given by

$$\Delta G_1 = \Delta G_1^c + \frac{2\gamma\, V_m}{S_1}$$

If it is assumed that the secondary cells consume the the remaining free energy during the growth because it grows considerably slowly as compared to the primary cells then,

$$\Delta G_2 = (1\text{-}p)\, \Delta G_0 - \left[\frac{2\gamma\, V_m}{S_1} - \frac{2\gamma\, V_m}{S_2} \right] \qquad (1.28)$$

Assuming that the secondary cells also follow Petermann and Hornbogen's growth kinetics

$$V_2 = -\frac{8\, D_b \delta}{RT\, S_2^2}\, \Delta G_2 \qquad (1.29)$$

Thus, from growth velocity, interlamellar spacing and the driving force ΔG_2 for the secondary cells, the diffusivity values can be calculated

1.7.8 Nickel Indium System

The Nickel-Indium phase diagram is complex with three eutectic, two peritectic, two eutectoid and four peritectoid reactions as shown in Fig 1.4

The maximum solubility of In in Ni was reported by Hellner [23] as 14.5 at % for the Ni-rich eutectic temperature at 910°C. The solubility of In in Ni drops to 0.002 at.% at room temperature according to E A. Peretti [22]

Ni_3In (θ) phase is DO_{19} type (face centered cubic) structure The reported lattice parameters are a = 5.320 A° and C = 4 242 A°. The super-saturated matrix (α_0) and the solute depleted α solid solution, both have simple FCC type structure

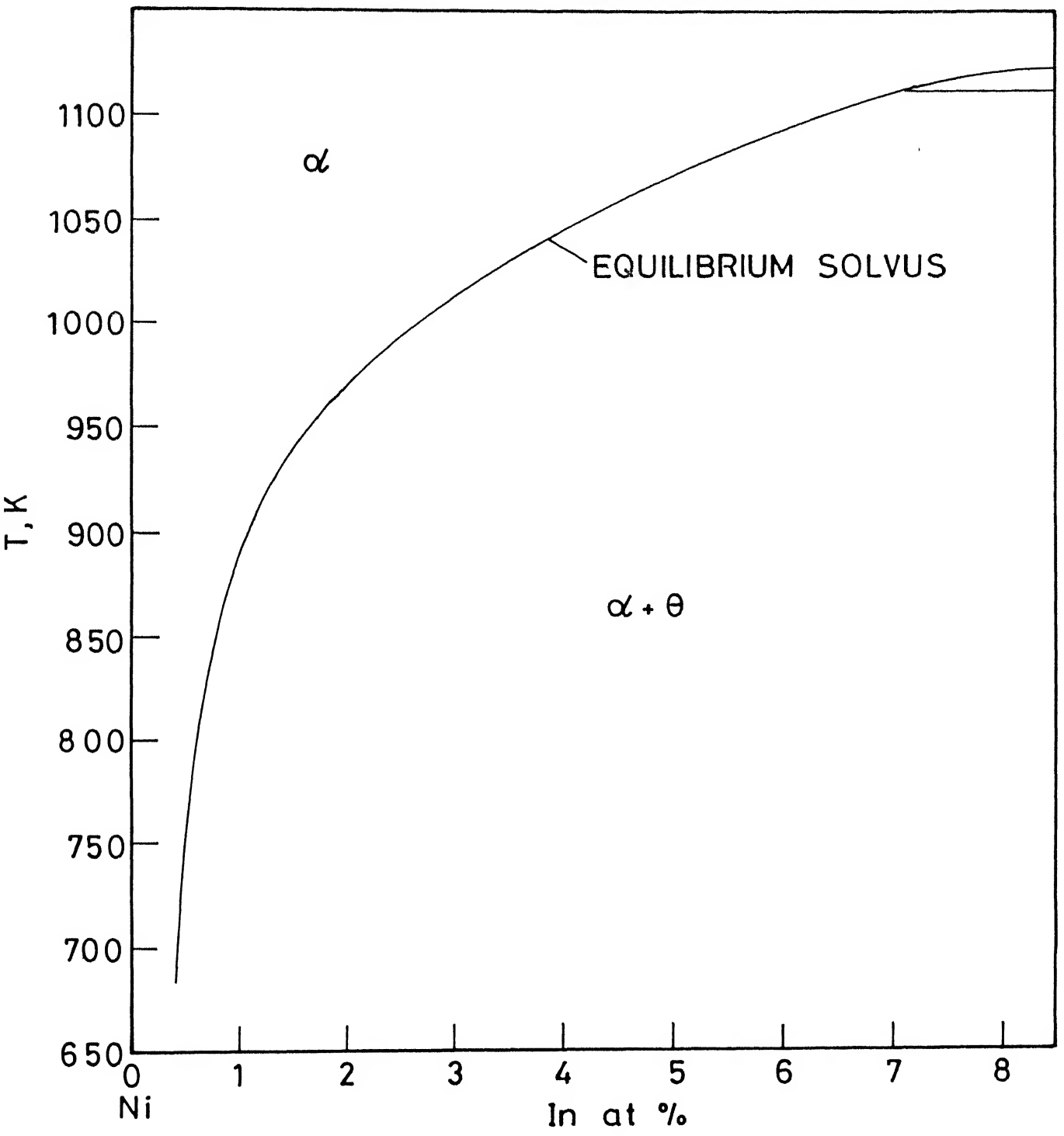

Fig.1.4 Ni-rich part of the Ni- In phase diagram.

Chapter 2. Experimental procedure

2.1 Preparation of the alloy

The experiments have been carried out for Ni - 4 at % In alloy which were prepared by appropriate amount of Nickel and Indium of four N purity The prepared alloy in shape of cylindrical rods were encapsulated in a quartz tube to avoid high temperature oxidation and given homogenisation treatment. Homogenisation of the alloy involves treating the alloy for 3 days at 850°C, followed by treatment at 900°C for one week and then finally treating the alloy at 950°C for another three days. To break the cast structure and to obtain polycrystalline structure, the alloy was thermally cycled between 950°C and 650°C Just after 950°C treatment, the alloy was transfered to the furnace held at 650°C for one hour followed by homogenisation again at 950°C for one day and quenched

The alloy thus prepared was cut into thin discs of 1- 2 mm thickness with the help of a hacksaw. The cut samples were ground lightly followed by cleaning in methanol and encapsulated in a quartz tube. The cut samples were again thermally cycled between 950°C and 650°C to relieve the stresses generated because of cutting as per the following schedule.

(i) 900°C for 1 hour

(ii) 650°C for 1 hour

(iii)900°C for 24 hour

2.2 Heat Treatment

In order to study the kinetics of discontinuous reactions the solution annealed samples were aged at ten temperatures from 737°C to 467°C with 30°C

interval at each temperature of treatment. All the treatments were done in salt bath maintained within ±2°C of the desired treating temperature. Aged samples were quenched in cold water

2.3 Metallography of Treated Samples

For metallographic examination, the aged samples, treated at different temperatures were mounted in a hot mounting press and polished carefully. The etchant used was a solution of anhydrous ferric chloride in ethyl alcohol in the ratio given below :

10% $FeCl_3$ in C_2H_5OH (90%)

2.3.1 Optical Microscopy

In order to determine the growth rate of primary and secondary cellular precipitate the width of the grain boundary precipitate in a direction perpendicular to the grain boundary was measured An average of fifty such measurements of each heat treated sample was taken to evaluate the growth rate.

2.3.2 Interlamellar Spacing

The interlamellar spacing of primary and secondary cells at each temperature was found by determining the number of lamellae present in a specific distance. Interlamellar spacing measurements of secondary cells at all the temperatures and few of the higher temperatures of primary cells were performed on optical microscopy, because of the lamellar spacing being on the higher side could be resolved easily. For low temperatures, the lamellar spacing of the primary cell were determined using a scanning electron microscope. Photographs taken on SEM were used to find out the above.

2.3.3 X - Ray analysis

The composition of the solute depleted α phase was determined for both primary and secondary cellular reaction by X-ray diffraction measurement on bulk specimens. A Cu K_α radiation and Ni filter were used. Each time, a fully annealed Ni - standard of four N purity was used to account for instrumental error. The 2θ values corresponding to the (220) peak were recorded at a scanning speed of 0.3° / min.

The precise lattice parameter was calculated and thereby from the composition - lattice parameter data reported by Singleton [23] was used to determine the composition.

Chapter 3. Results And Discussion

3.1 Morphology

The microstructure observed primarily through optical microscopy revealed that the Ni-In solid solution decomposed into α and θ phases by discontinuous precipitation at all the aging temperatures in the range of 770K to 1010K The nucleation of Ni_3In lamellae occured at the grain boundary Fig 3·1 The primary cell growth occured by multiplication of lamellae both by branching and nucleation of new lamellae at the cell boundary front. There appears to be no well defined habit plane for the θ precipitate in the more or less continuous α phase because the lamellae change direction frequently as they grow. This might be expected as there exists rather large atomic mismatch of the order of 5% along the closed packed directions for the α and θ phases. After or even somewhat before the primary reaction has completely decomposed the super-saturated α_0 phase, a secondary reaction begins to decompose the lamellar product of primary reaction into the same lamellar structure but with a higher spacing (Fig 3·2)

3·2 Growth Rate

To determine the growth rate of primary and secondary cells, growth distance of the cellular precipitate was measured at different intervals of time at each temperature. About fifty measurements were made from different regions of each specimen and the growth distance data averaged The average of growth distance data multiplied by $\frac{\pi}{4}$ to be consistent with the bulk averaging technique used by Gust etal. [24]. It averages all orientations of cells, nucleating from grain boundaries of different misorientation. At each temperature, the growth rate of

Fig. 3·1 Optical photomicrograph of primary cellular precipitate, sample aged at 800 K for 10 hrs at 500X magnification.

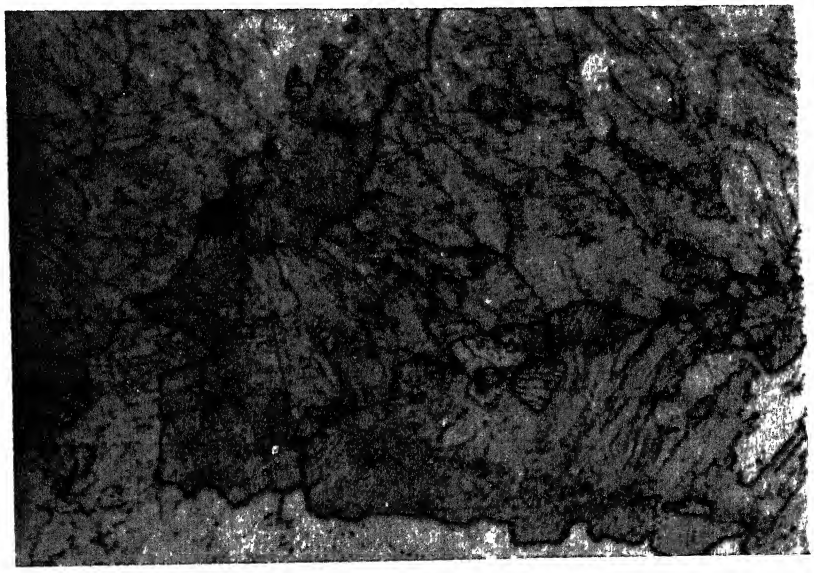

Fig. 3·2 Optical photomicrograph of secondary cellular precipitate, sample aged at 800 K for 150 hrs at 500X magnification.

both primary and secondary cells were determined from the average growth distance versus time plot. The primary and secondary growth rates are shown in Table 3·1 and Fig. 3·3 against the temperature of aging As can be seen in Fig. 3·3, the velocity of the reaction front V_1 for primary reaction exhibits typical 'C' curve behaviour i.e it initially increases with increasing aging temperature, reaches a maximum at about 940K and then decreases The values are in good agreement with those of Chuang etal. [7], Abdou [6] and Gupta etal [8] The cell front velocity V_2 for secondary reaction also exhibits typical "C" curve behaviour and has its peak at 950K. The cell growth rates of the secondary reaction cells are about two order of magnitude lower than those of primary cells at all aging temperatures. The much slower growth rate is the result of the fact that driving force for the secondary reaction is much smaller than that for the primary reaction while the lamellar spacing is larger

3·3 Interlamellar Spacing

The interlamellar spacing data for primary and secondary cells (S_1 and S_2 respectively) are presented in Table 3·1 and plotted in Fig. 3·4. Each data point is the average of fifty measurements made randomly on the specimens and multiplied by $\frac{\pi}{4}$ to be consistent with the average growth rate from the bulk specimen. The interlamellar spacing decreases continuously with decreasing temperature of aging as expected. The decrease in interlamellar spacing is higher at higher aging temperatures and more or less constant at lower temperatures of aging. The interlamellar spacing of secondary cells are 2 - 4 times of the values observed for the primary cells.

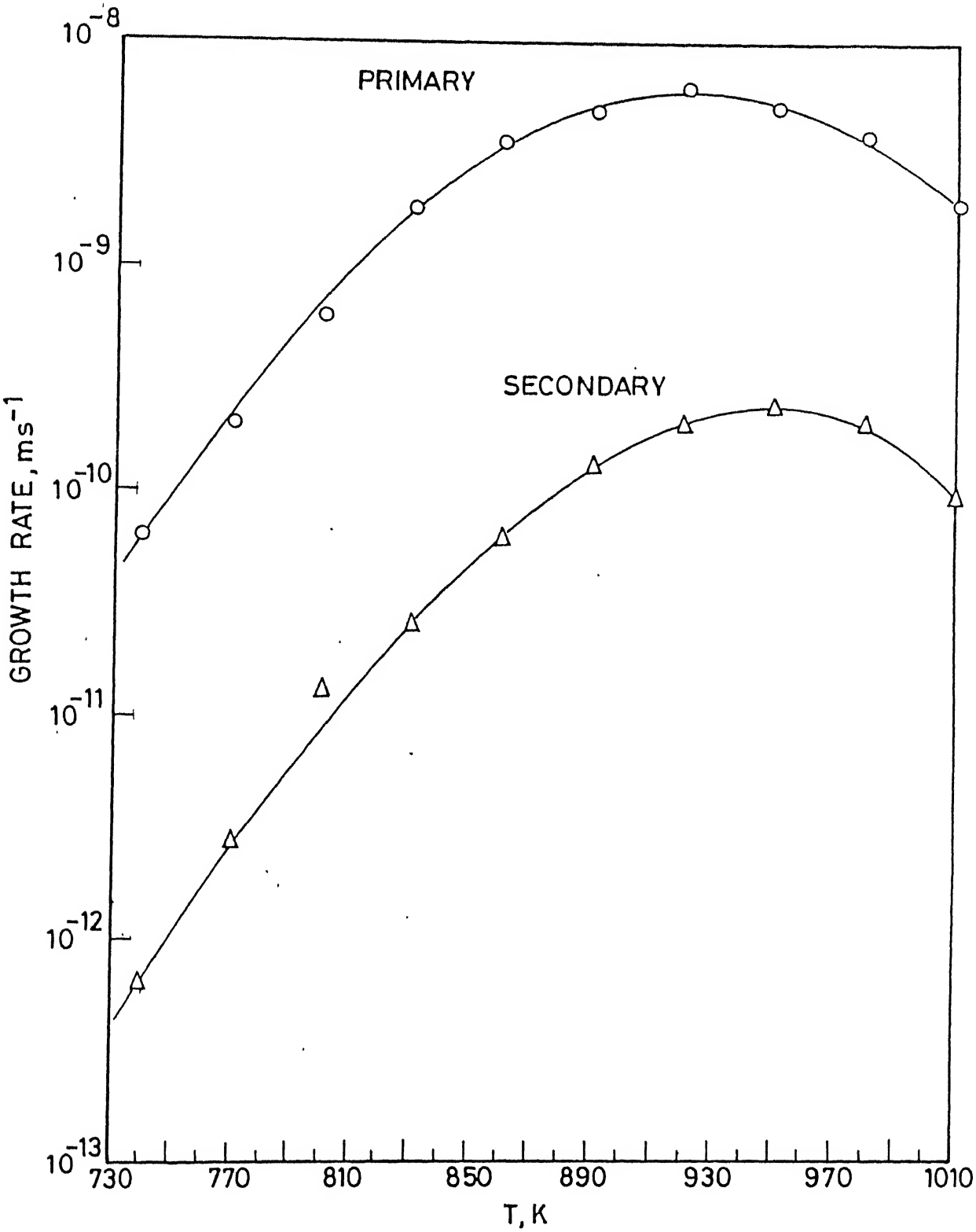

Fig. 3.3 Growth Rate Vs Temperature.

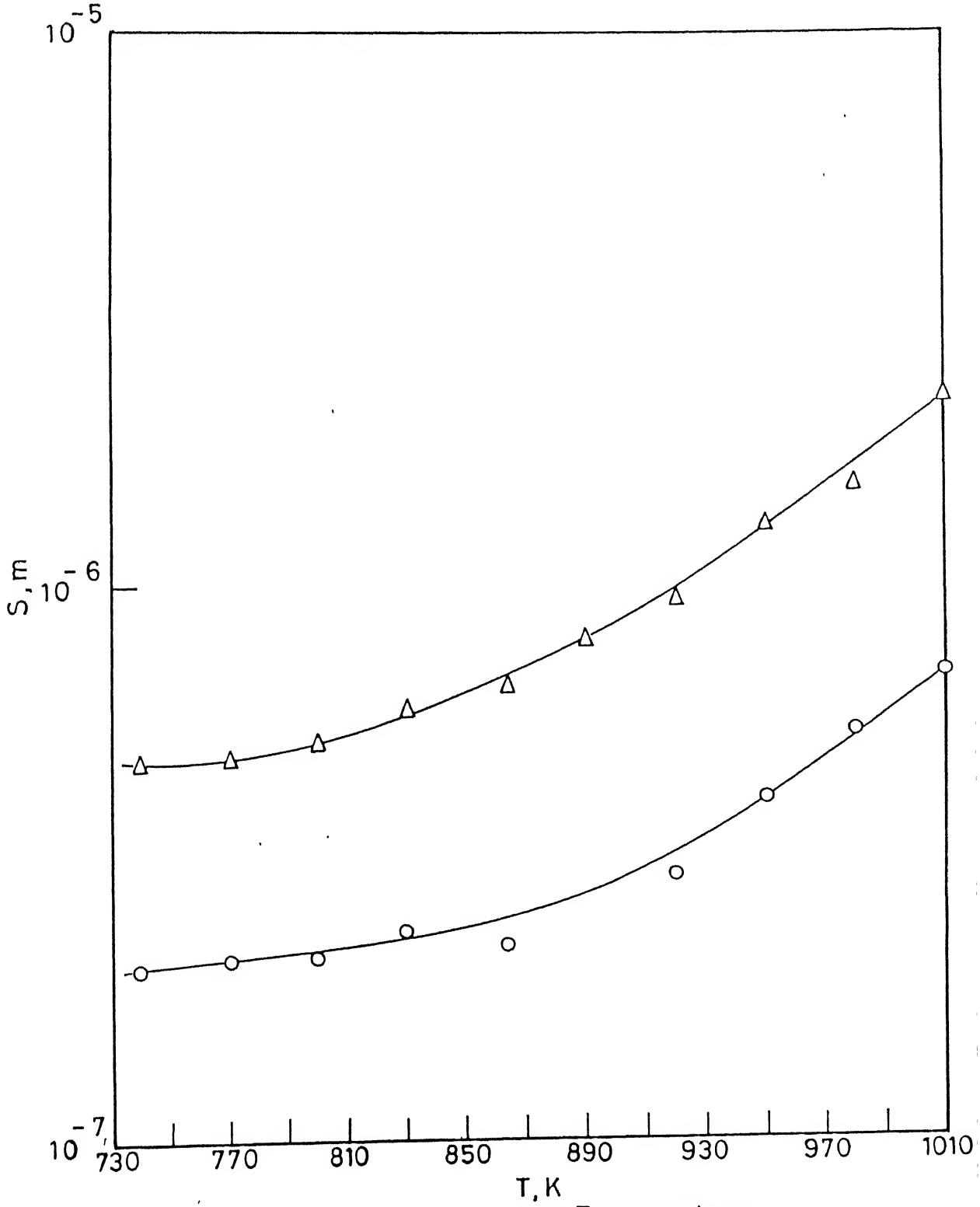

Fig.3.4 Interlamellar Spacing Vs Temperature.

3·4 The Composition of the Depleted Matrix

The average composition of α-phase in primary and secondary cells were determined from the lattice parameter measurements using X-ray diffraction and are shown in Table 3·1 and plotted in Fig. 3·5 along with the recently published equilibrium phase diagram of Ni - rich side of the system [7] The diagram differs substantially from those published by Hansen and Anderko [25] and Massalski etal [26]. The composition of the depleted α-phase of primary cells, ${}^{P}X_{B}^{\alpha}$ was determined from the specimen containing about 90-95% primary cells and the remaining secondary cells and untransformed regions It is to be noted that since secondary cells appear after about 60-70% of the transformation of the supersaturated solid solution is completed, the products of secondary reactions are expected to be present in the microstructure as minor constitutent at the termination stage of the primary reaction and therefore cannot be avoided

The composition of the depleted α-phase of the secondary cells ${}^{S}X_{B}^{\alpha}$ was determined from specimens containing about 90-95 % secondary cells and the remaining primary and tertiary cells. At the termination stage of the secondary reaction, tertiary cells appear and therefore cannot be avoided.

Ignoring small deviations at some temperatures, the composition values of the α-phase with the secondary cells follow the equilibrium solvus very well. The α-phase of the primary cells is richer in In at all temperatures as observed for other alloy systems undergoing cellular precipitation

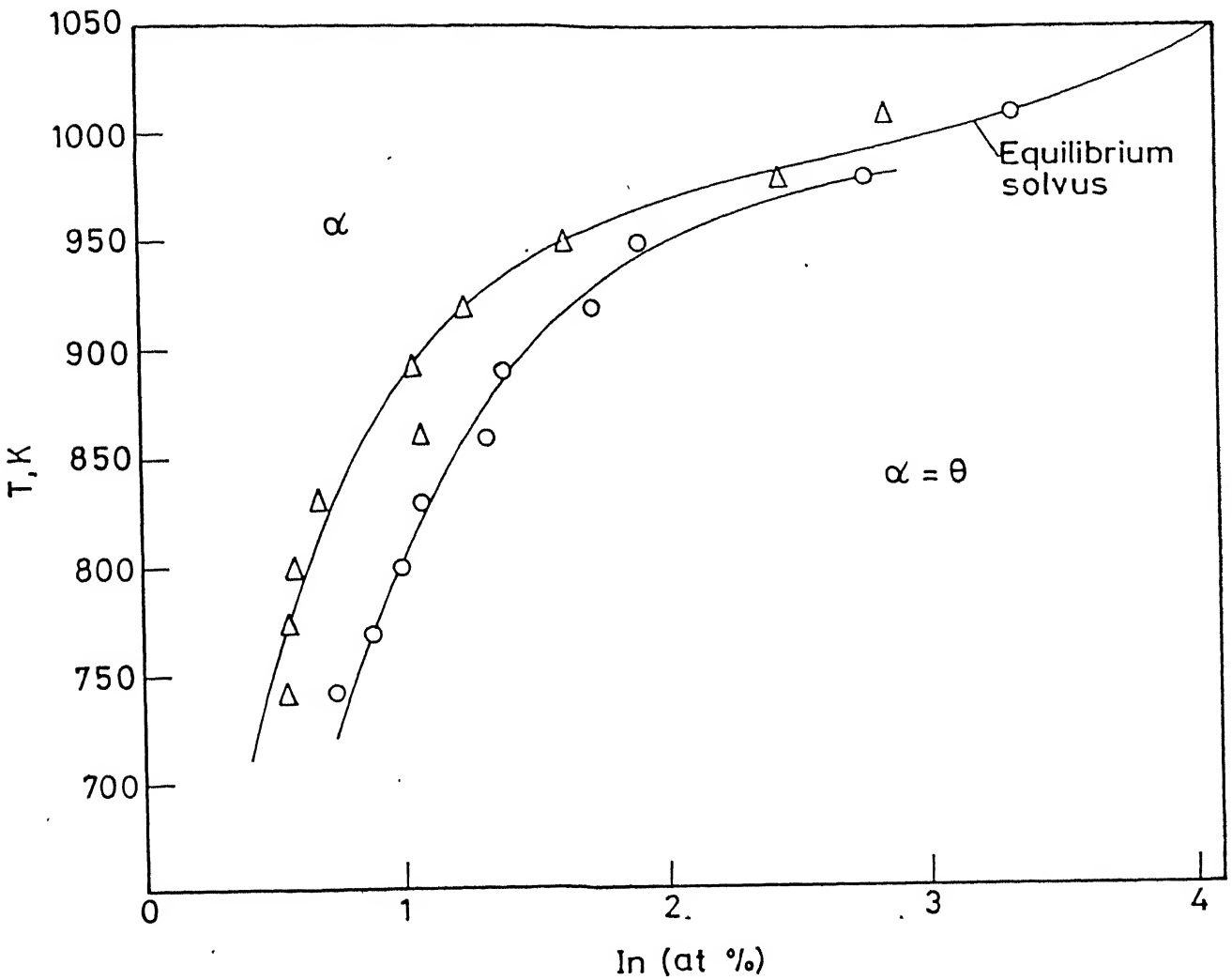

Fig. 3.5 Composition of the depleted matrix.

Table 3·1 : Growth Rate, Interlamellar Spacing And Composition Data During Growth of Primary And Secondary Cell.

T (K)	V_1	V_2	S_1	S_2	${}^{e}X_B^{\alpha}$	${}^{P}X_B^{\alpha}$	${}^{S}X_B^{\alpha}$
	(ms^{-1})		$(10^{-8}$ m)	$(10^{-8}$ m)			
1010	$1.83X10^{-9}$	$0.939X10^{-10}$	69 85	217 37	0 0290	0 0333	0 0285
980	$3.67X10^{-9}$	$2\ 03X10^{-10}$	54 56	149 78	0.0220	0 0257	0 0243
950	$5.0X10^{-9}$	$2\ 35X10^{-10}$	41.25	121 89	0.0165	0 0190	0 0162
930	$6.15X10^{-9}$	$1.96X10^{-10}$	30 23	94 72	0 0125	0 0173	0 0124
890	$4.75X10^{-9}$	$1.3X10^{-10}$	27 86	80 74	0 0102	0 0139	0 0104
860	$3\ 49X10^{-9}$	$6.18X10^{-11}$	22.56	66 04	0 0085	0 0132	0 0107
830	$1.77X10^{-9}$	$2.56X10^{-11}$	24.06	60.45	0.0072	0 0107	0 0067
800	$5.75X10^{-10}$	$1.32X10^{-11}$	21.57	52.25	0 0061	0 0100	0 0057
770	$1.96X10^{-10}$	$2.73X10^{-12}$	21 28	49.16	0.0055	0 0088	0 0054
740	$6.33X10^{-10}$	$6.4X10^{-13}$	20 59	48.00	0 0049	0 0074	0.0054

3·5 Kinetics Of Primary Cellular Reaction

A number of theories have been proposed to describe the cellular phase transformation (Section 1·8) in substitutional alloys In most of these theories growth rate is related to the boundary diffusivity and interlamellar spacing by the following equation

$$V_i = \alpha \frac{KD_b\delta}{S_i^2} \qquad (3\ 1)$$

where α is related to the composition of the depleted matrix and has different values for different models. The value of the parameter α for the Petermann and Horbogen [13] theory is

$$\alpha = - \frac{8\ \Delta G_i}{RT} \qquad (3\ 2)$$

where ΔG_i is the driving force used for primary cell growth and RT have their usual meaning. The driving force for primary cellular reaction was calculated from the relation.

$$\Delta G_i = \Delta G_i^{C} + \Delta G_i^{\gamma} \quad \left(= \frac{2\gamma V_m}{S_i} \right) \qquad (3\ 3)$$

where ΔG_i^{C} is the chemical free energy available for the growth of primary cells and γ is the interfacial free energy of α/θ interface The interfacial energy of Ni - In alloy is not available in the literature and is taken to be 500 MJm^{-2} as used by Chuang etal. [7]. The driving force for the cellular precipitation reaction has been calculated using the regular solution model. Accordingly,

$$\Delta G_0^{\alpha} = RT \left({}^{P}X_A^{\alpha} \ln {}^{P}X_A^{\alpha} + {}^{P}X_B^{\alpha} \ln {}^{P}X_B^{\alpha} \right) + LRT\ {}^{P}X_A^{\alpha}\ {}^{P}X_B^{\alpha} \qquad (3.4)$$

From the known values of the free energy of formation of the θ phase [27], the value of L has been determined at each temperature using procedure outlined by Fournelle [19] and the equation

$$L = \frac{\frac{\Delta G^{\theta}}{RT} - \left(X_B^{\beta} \ln {}^{e}X_B^{\alpha} + X_A^{\theta} \ln X_A^{\alpha} \right)}{({}^{e}X_B^{\alpha})^2 + X_B^{\theta} (1 - 2 X_B^{\alpha})} \qquad (3.5)$$

where X_B^{θ} is the fraction of In in the θ phase (= 0.25) and ${}^{e}X_B^{\alpha}$ is the equilibrium composition at the aging temperature and is given in Table 3.1. Using the value of L, thus obtained (Table 3.2) the free energy of the (α + θ) phase mixture, $\Delta G_1^{\alpha+\theta}$, of the primary cells has been obtained at each temperature at the original alloy composition from the relation

$$\Delta G_1^{\alpha+\theta} = \left(\frac{X_B^{\theta} - {}^{1}X_B^{\alpha}}{X_B^{\theta} - {}^{P}X_B^{\alpha}} \right) \Delta G_1^{\alpha} + \left(\frac{{}^{P}X_B^{\alpha} - {}^{P}X_B^{\alpha}}{X_B^{\theta} - {}^{P}X_B^{\alpha}} \right) \Delta G^{\theta} \qquad (3.6)$$

The above has been obtained from application of Lever rule to free energy of phase mixtures. The chemical free energy of the primary reaction is determined from the relation,

$$\Delta G_1^{C} = \Delta G_1^{\alpha+\theta} + \Delta G_0^{\alpha} \qquad (3.7)$$

where ΔG_0^{α} is the value of ΔG^{α} at the original alloy composition.

Typical free energy - composition diagrams used for the calculation of the driving force for the growth of primary cells are shown at 800K and 980K in Fig 3.6 (a) and (b). The chemical free energy and the available driving force for the primary reaction are shown in Table 3.2

The Hillert [11] model was also used to analyse the data of the present investigation. Accordingly, the value of 'α' in equation (3.1) is

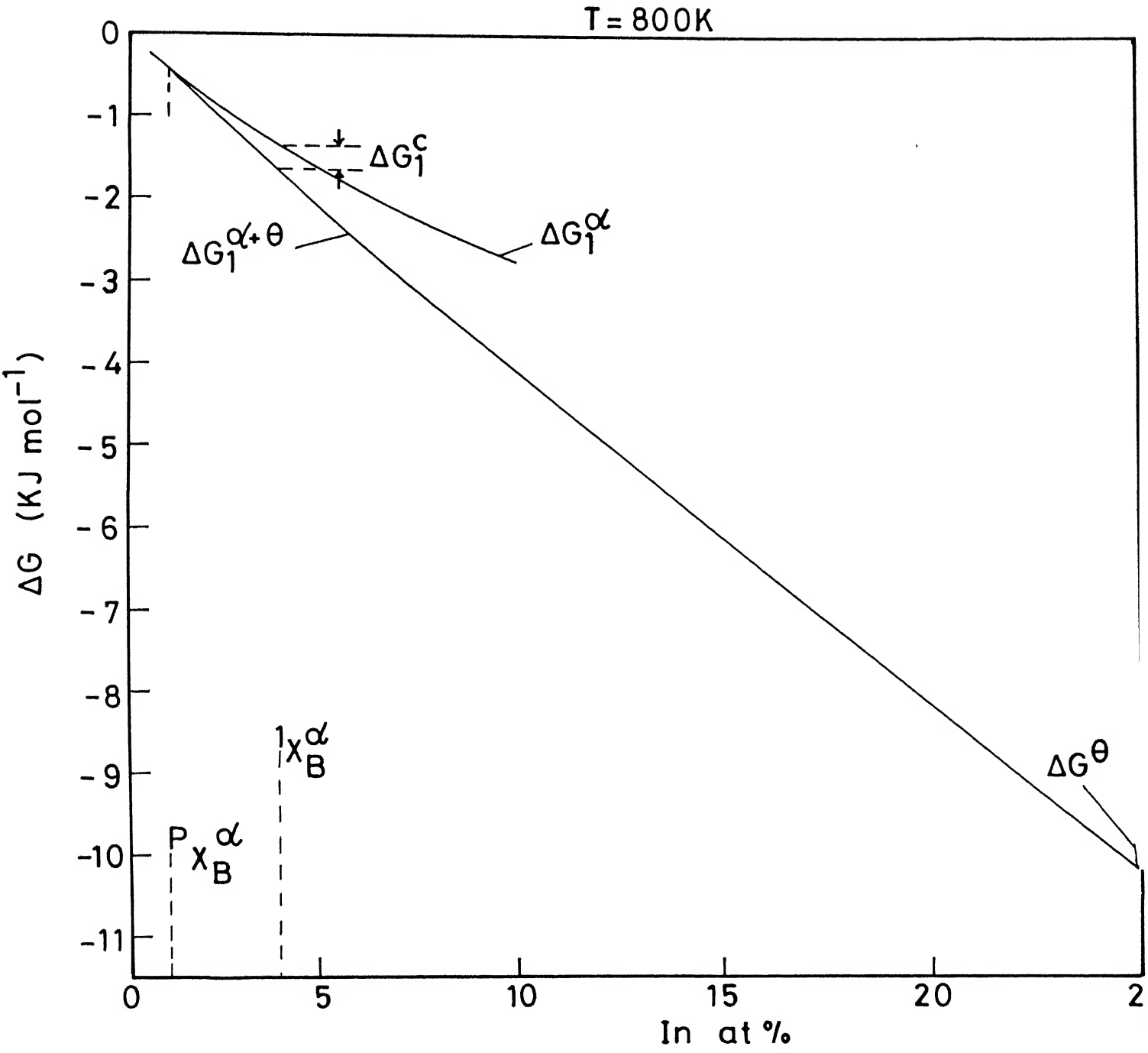

Fig. 3.6(a) Free energy-composition diagram at 800K.

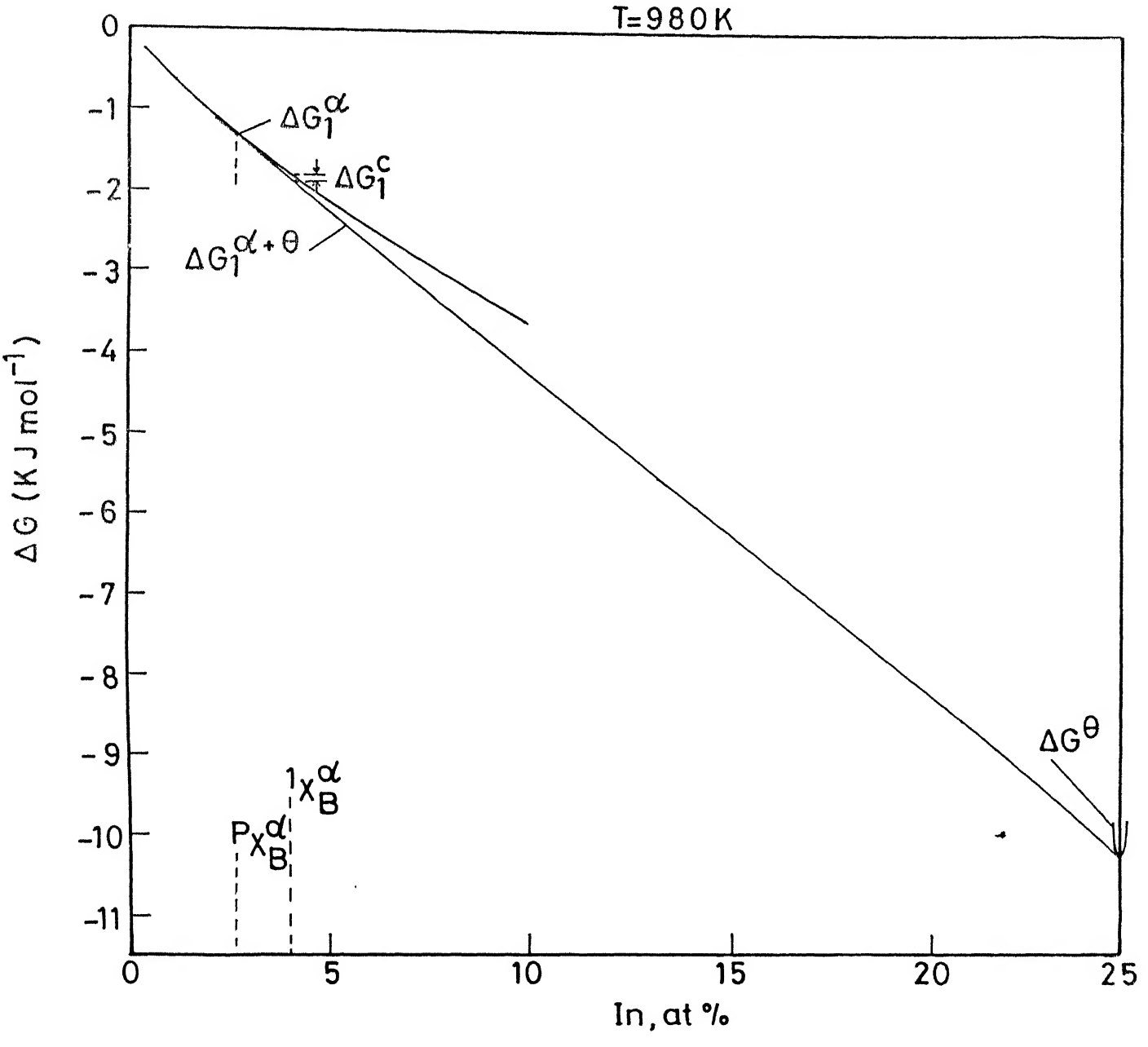

Fig. 3.6(b) Free energy-composition diagram at 980K.

$$\alpha = \frac{8S_i}{S_i^{\alpha}} \left(\frac{X_B^{\alpha} - X_B^{\alpha/\theta}}{{}^{i}X_B^{\alpha} - X_B^{\alpha}} \right) \tag{3.8}$$

where X_B^{α} is the variable composition of the α phase and $X_B^{\alpha/\theta}$ is the interface composition Taking $L^{\alpha} = L^{\theta} = 0.5$ and $K^{\alpha} = 1$ as suggested by Hillert [11], a modified value of the parameter

$$\alpha = \frac{4S_i}{S_i^{\alpha}} \tag{3.9}$$

since L^{α}, L^{θ} and K^{α} values are not known, substitution of $X_B^{\alpha/\theta} = {}^{e}X_B^{\alpha}$ and $X_B^{\alpha} = {}^{P}X_B^{\alpha}$ yields a modified value for α , which is given as

$$\alpha = \frac{8S_i}{S_i^{\alpha}} \left(\frac{{}^{P}X_B^{\alpha} - {}^{e}X_B^{\alpha}}{{}^{i}X_B^{\alpha} - {}^{P}X_B^{\alpha}} \right) \tag{3.10}$$

The value of α for the theory of cellular precipitation after Cahn [9] is

$$\alpha = 4\eta \tag{3.11}$$

where η is related to the fraction of supersaturation recovered by the following equation

$$W = \frac{{}^{i}X_B^{\alpha} - {}^{P}X_B^{\alpha}}{{}^{i}X_B^{\alpha} - {}^{e}X_B^{\alpha}} = \frac{\tanh \sqrt{\eta}}{\sqrt{\eta}} \tag{3.12}$$

The diffusivity during the primary cell growth after Turnbull [10] is also given by equation (3·1) and the parameter α is

$$\alpha = \frac{{}^{i}X_B^{\alpha} - {}^{e}X_B^{\alpha}}{{}^{i}X_B^{\alpha}} \tag{3.13}$$

The value of α for the model after Sundquist [12] is $4\eta\overline{\cos\theta}$ and η is determined from the relationship

$$W = \frac{{}^{i}X_B^{\alpha} - X_B^{\alpha(0)}}{{}^{i}X_B^{\alpha} - {}^{e}X_B^{\alpha}} = \frac{\tanh\sqrt{\eta}}{\sqrt{\eta}} \qquad (3\ 14)$$

where $X_B^{\alpha(0)}$ is the solute concentration at the three phase junction $\alpha/\alpha_0/\theta$ and is given as

$$X_B^{\alpha(0)} = {}^{e}X_B^{\alpha} \exp\left[\frac{2\gamma V_m \theta\,(\,X_B^{\theta} - {}^{i}X_B^{\alpha}\,)}{RT\ s_i^{\alpha}\ W\,(\,{}^{i}X_B^{\alpha} - {}^{e}X_B^{\alpha}\,)}\right] \qquad (3\ 15)$$

From the Gibbs - Thomson's equation

$$W = \frac{{}^{i}X_B^{\alpha} - {}^{P}X_B^{\alpha}}{{}^{i}X_B^{\alpha} - {}^{e}X_B^{\alpha}} \quad \text{and} \quad \theta = \frac{\pi}{6}$$

From the experimentally determined values of the growth rate , interlamellar spacing and composition of the depleted matrix of the primary cells , the $KD_b\delta$ values were calculated at each aging temperature for the above five models and the values are presented in Table 3·3 (a) and (b). The temperature dependence of the diffusivity is shown in Fig. 3·7 (a) and (b).

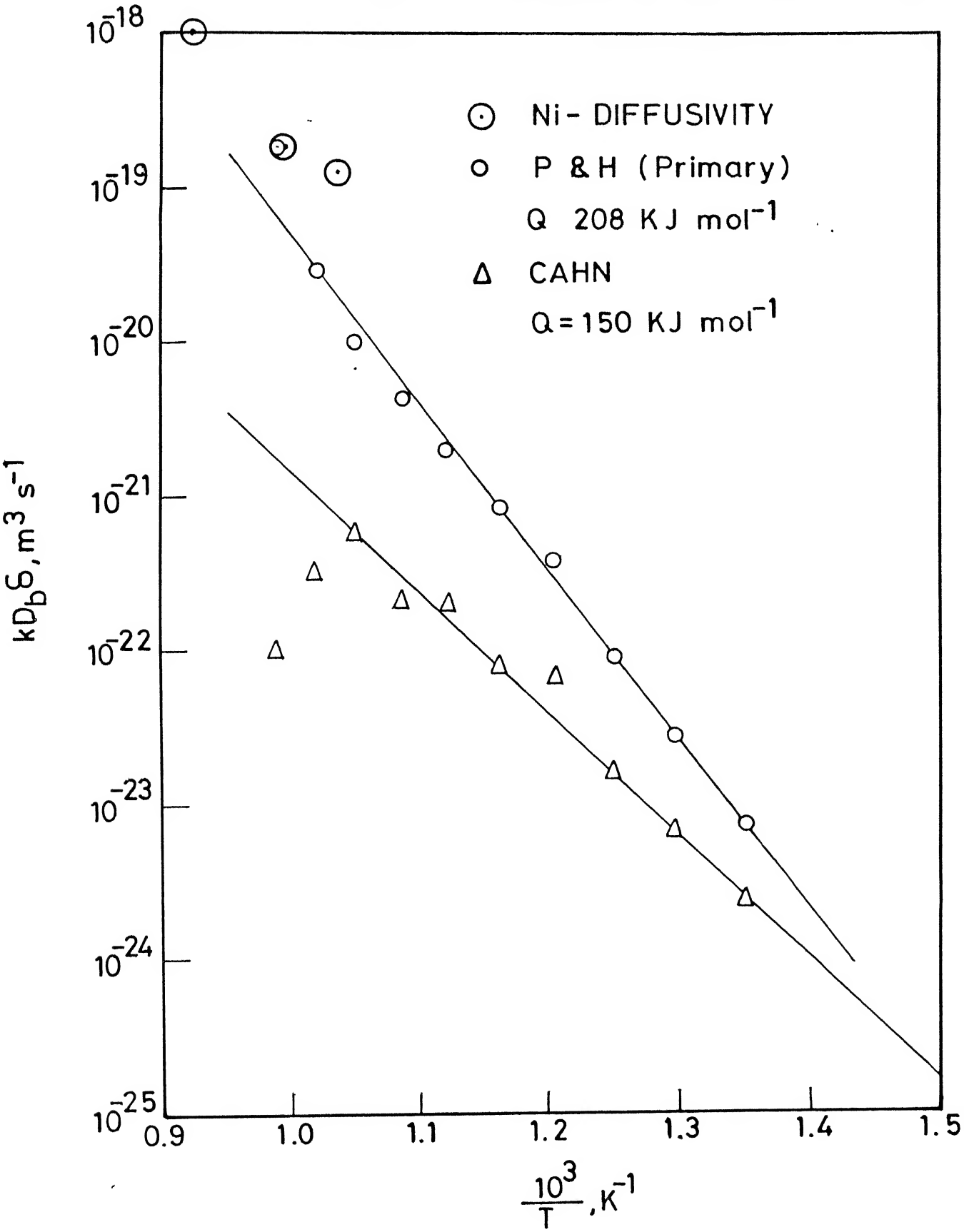

Fig. 3.7 (a) $kD_b\delta$ Vs Temperature.

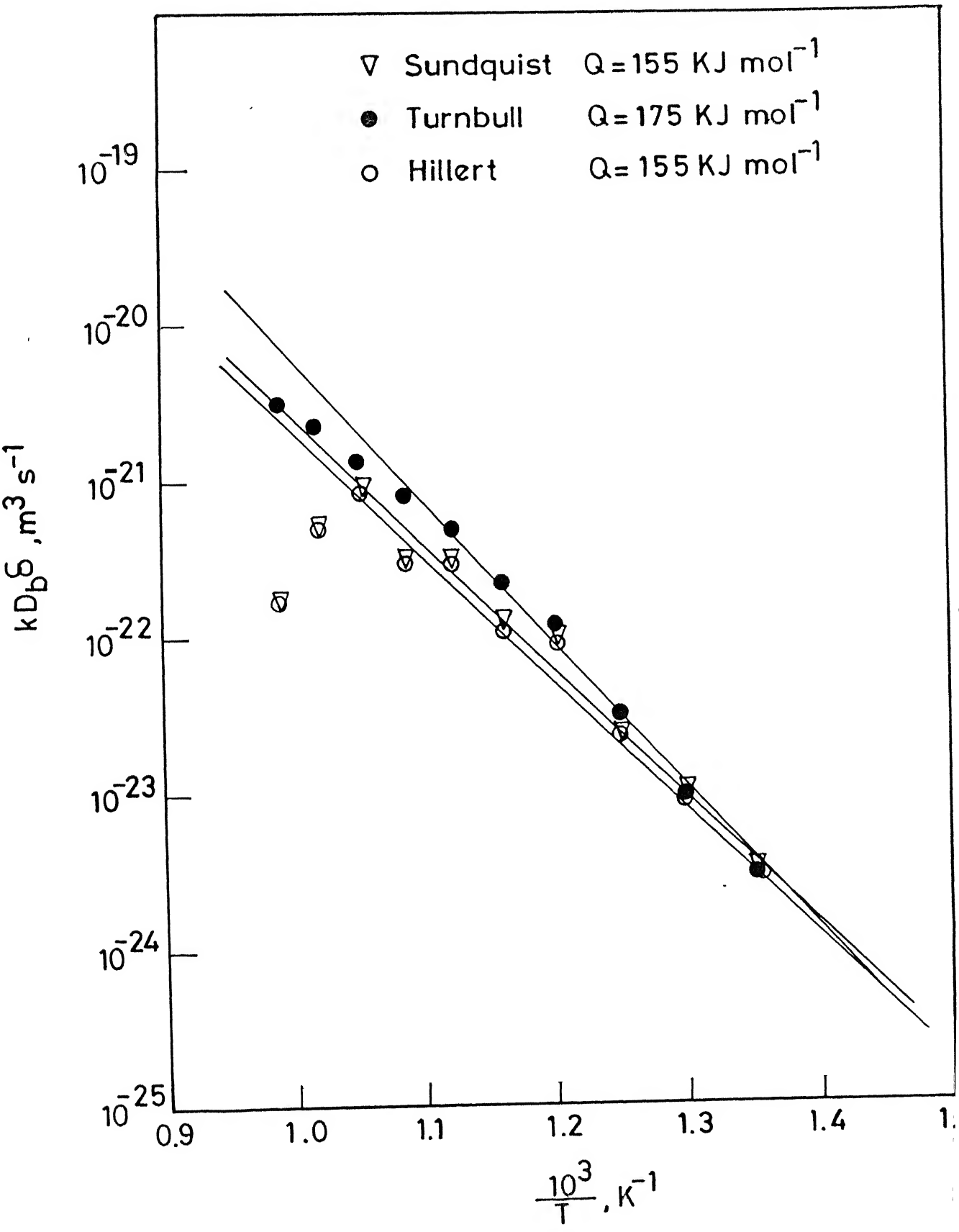

Fig. 3,7 (b) $kD_b\delta$ Vs Temperature.

Table 3·2 : Chemical free energy, Interfacial free energy and the driving force for the growth of primary and secondary reaction. All values are in J mol^{-1}.

T (K)	$-\Delta G_1^{\alpha}$	$-(\Delta G_2^{\alpha+\theta} - \Delta G_0^{\alpha})$	$-\Delta G_2^{\alpha}$	- L	ΔG_1^{γ}	ΔG_2^{γ}	$-\Delta G_1$	$-\Delta G_2$
740	310 70	313 55	2 85	1.19723	33 17	14 23	277 52	21 79
770	294.70	299 45	4.75	1.09833	32.09	13 83	262.60	22 95
800	280.20	286.33	6.13	1.00324	31.66	13.07	248 53	24.72
830	253.49	257.97	4.48	0.98488	28 39	11 30	225 10	21 57
860	221.05	226 60	5.55	0.97934	30 27	10.34	190 77	25 47
890	189.78	193.87	4.09	1.00165	24 51	8 46	165.26	20 14
920	148.66	154 58	5.92	1 05555	22 59	7 21	126 06	21 30
950	100 22	101.57	1.35	1.19458	16 55	5 60	83.67	12.30
980	50.66	52.15	1.49	1 35395	13 48	4.56	37.17	10.41
1010	14.93	17.66	2.73	1 51171	9 78	3 14	5 1515	9.37

Table 3.3 (a) $KD_b\delta$ values for primary cell growth

$^1\chi_B^{\alpha} = 0.04$, $V_m = 6.83 \times 10^{-10}$

T (K)	P & H	Cahn	Turnbull	Hillert	Sundquist
740	7.436E-24	2.386E-24	3.015E-24	3.155E-24	3.520E-24
770	2.705E-23	6.846E-24	1.029E-23	9.133E-24	1.0133E-23
800	9.260E-23	1.729E-23	3.266E-23	2.329E-23	2.552E-23
830	3.926E-22	6.979E-23	1.249E-22	9.409E-23	1.035E-22
860	8.321E-22	7.932E-23	2.255E-22	1.1227E-22	1.2088E-22
890	2.063E-21	2.1066E-22	4.948E-22	2.899E-22	3.150E-22
920	4.262E-21	2.123E-22	8.175E-22	2.998E-22	3.170E-22
950	1.004E-20	5.815E-22	1.4481E-21	8.121E-22	9.048E-22
980	2.917E-20	3.340E-22	2.427E-21	4.941E-22	5.182E-22
1010	1.819E-19	1.019E-22	3.246E-21	1.685E-22	1.711E-22

Note All $KD_b\delta$ values for the various models are in m^3s^{-1}

Table 3.3 (b) $KD_b\delta$ values for secondary cell growth

$^{i}X_B^{\alpha} = 0.04, \qquad V_m = 6.83 \times 10^{-10}$

T (K)	P & H	Livingston and Cahn
740	5.2E-24	5.655E-23
770	2 3E-23	2.739E-22
800	1.27E-22	1.433E-21
830	3.74E-22	3 497E-21
860	9.45E-21	5 097E-21
890	3.89E-21	2.135E-20
920	7.89E-21	3.80E-20
950	2 8E-20	7.459E-20
980	4.45E-20	6.520E-20
1010	4.97E-20	5.091E-20

Note : All $KD_b\delta$ values for the various models are in m^3s^{-1}

Except at few high temperatures, the data follow a linear behaviour within the experimental error, for all models in the whole range of temperatures

The activation energy Q has been calculated for the five models and shown in Table 3·4 .

The activation energy values lie within ± 20% of the average value of all the models. The $KD_b\delta$ values for the diffusion of In along symmetric 39° <011> – {011} tilt grain boundaries in Ni have been reported by Gust etal. [28] from diffusion studies at three temperatures as shown in Fig 3·7 (a). Although the activation energy Q (= 166 kJ mol^{-1}) is different from the result obtained in the present investigation, the diffusivity values are in good agreement in the temperature range of diffusion studies.

The activation energies for solute diffusion along a grain boundary (Q_b) in the presence of a strongly segregating solute (Q_b^{seg}) are related by the following equation [29]

$$Q_b^{seg} = Q_b + N\alpha' a^2 \Delta\gamma_{gb} \qquad (3.16)$$

where N = Avogadro's number

α' = structure factor for vacancy controlled diffusion substitutional solute.

a = atomic size

$\Delta\gamma_{gb}$ = difference in the grain boundary energy in the presence of a strongly segregating solute

Equation (3.15) illustrates that Q_b^{seg} will be higher because $\Delta\gamma_{gb}$ will be higher, the stronger the tendency for segregation of solute at the grain boundary. An increase of Q_b from 157 to 180 kJ mol^{-1} has been predicted in case of $\frac{1}{5}$ monolayer of Sb in Cu. A higher fraction of segregated monolayer of solute is

expected at the grain boundaries in moderately dilute alloys with higher solute concentration

Table 3·4 : Activation Energy values for different theories

MODEL	Activation energy (kJ mol^{-1})
Petermann and Hornbogen (Primary)	208
Turnbull	175
Sundquist	155
Hillert	155
Cahn	150
Petermann and Hornbogen (Secondary)	220
Livingston and Cahn	204

The γ_{gb} would increase with increasing density of segregation resulting into higher activation energy for solute diffusion through the grain boundaries. This explains to some extent higher activation energy for solute diffusion through grain boundaries during cellular precipitation. The diffusivity values observed experimentally are about seven orders of magnitude higher than the volume diffusivity at all temperatures. It can therefore be concluded that the growth of primary cells occurs by the diffusion of In along the grain boundaries.

3.5 Secondary Cell Growth Kinetics

The theory of discontinuous coarsening of cellular precipitate is based on the theory of primary cell growth after Petermann and Hornbogen [13]. The rate of growth of secondary cell is given by

$$V_2 = -\frac{8KD_b\delta}{RTS_2^2}\Delta G_2 \qquad (3.17)$$

where ΔG_2 is the driving force for the discontinuous coarsening reaction and is given by

$$\Delta G_2 = \Delta G_2^{C} - \Delta G_1^{C} + (\Delta G_2^{\gamma} - \Delta G_1^{C}) \qquad (3.18)$$

where ΔG_2^{C} is the chemical free energy available for the secondary cell growth, a part of which ($\Delta G_1^{C} + \Delta G_1^{\gamma}$) is used up for the primary cell growth and ($\frac{2\gamma V_m}{S_2} = \Delta G_2^{\gamma}$) remains with α/θ interface of the secondary cells. ΔG_2^{C} was calculated from the equation,

$$\Delta G_2^{C} = RT\left[{}^{i}X_B^{\alpha} \ln \frac{{}^{s}X_B^{\alpha}}{{}^{i}X_B^{\alpha}} + {}^{i}X_A^{\alpha} \ln \frac{{}^{s}X_A^{\alpha}}{{}^{i}X_A^{\alpha}} \right] \qquad (3.19)$$

As seen in Table 3·2, the chemical free energy values are very small, the maximum being – 6.13 J mol^{-1} at 800K. by using equation (3·18), the driving force used for the secondary cell growth was calculated and is presented in Table 3·2 From experimental growth and interlamellar spacing and the driving force, the $KD_b\delta$ was calculated at each temperature. The Arrhenius plot of Fig 3·8 represents the kinetics of secondary coarsening. The data points are well represented by a straight line. From the slope of the straight line, an activation energy of 220 kJ mol^{-1} is obtained which is in agreement with the value obtained for the primary cell growth.

Since the chemical free energy remaining after the primary cell growth is very small, the major contribution to driving force for the secondary cell growth stems from the difference in the interfacial free energies associated with the primary and secondary cells. The theory of discontinuous coarsening of the primary cells after Livingston and Cahn [20] proposes the above differences in the interfacial free energies to be the driving force Accordingly, the diffusivity is related to the growth rate and interlmellar spacing by the following equation :

$$KD_b\delta = \frac{V_2 (f_2^{\alpha})^2 f_2^{\theta} (X_B^{\theta} - {}^{s}X_B^{\alpha}) S_2^2 S_1 RT}{8\gamma V_m {}^{s}X_B^{\alpha} (1-\frac{S_1}{S_2})} \qquad (3\ 20)$$

The diffusivity was calculated at each temperature and is shown in Fig 3·8 Leaving out few high temperatures, the experimental data points are reasonably well represented to follow a straight line. The activation energy Q (= 204 $kJmol^{-1}$) obtained for the growth of secondary cells is comparable to the value obtained for the primary cell growth after Turnbull [10], Petermann and Hornbogen [13], and Cahn [9].

The diffusivity data matches well with the data obtained from the grain boundary diffusion studies of In in Ni. The diffusivity observed experimentally is

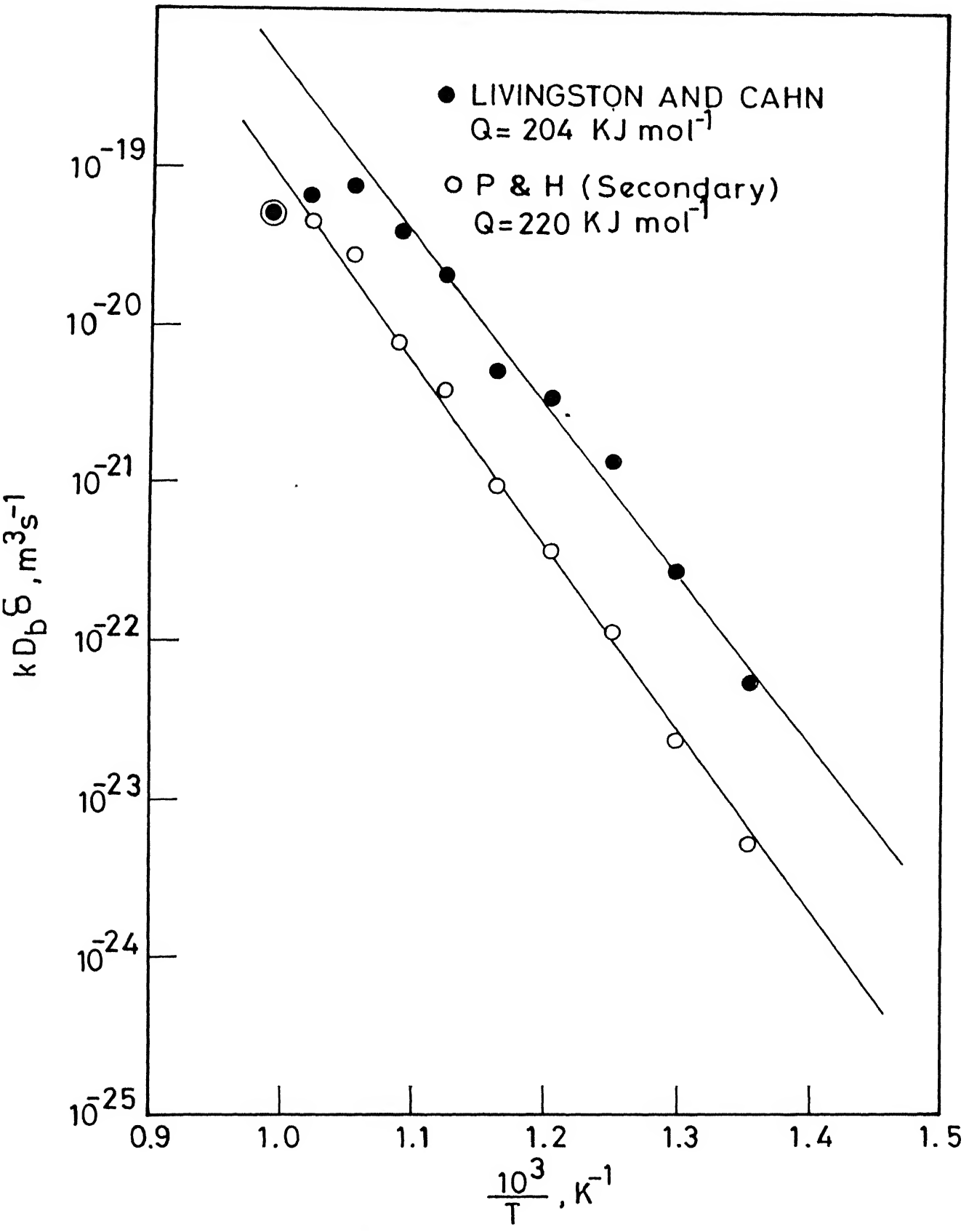

Fig 3.8 $kD_b\delta$ Vs Temperature.

about seven orders of magnitude higher than the volume diffusivity at each temperature. It can therefore be concluded that the growth of the secondary cell occurs by the addition of In along advancing grain boundaries

3.6 Mobility of the grain boundary

The analysis of the primary and secondary cellular growth kinetics can be extended by assuming a mobility controlled boundary migration Assuming a linear relationship to describe the cell boundary migration.

$$V = -\frac{M\Delta G}{V_m} \qquad (3\ 21)$$

where M is the mobility of the grain boundary. The mobility of the cell boundaries for both the primary and secondary cells are shown in Fig 3·9 and data is presented in Table 3·5. The Arrhenius plot of Fig. 3·9 describes the kinetics of cellular precipitation and discontinuous coarsening of cellular precipitate quite well. Except at high temperatures, the data fall on straight lines The activation energies are 191.4 and 192.3 $kJmol^{-1}$ for primary and secondary reaction respectively. These values are lower than those observed from the diffusivity data of primary and secondary cells and are about 0.7 times the activation energy for volume diffusion of In in Ni, thus supporting the earlier conclusion that the growth of cellular precipitate and its discontinuous coarsening is controlled by solute transfer through grain boundaries.

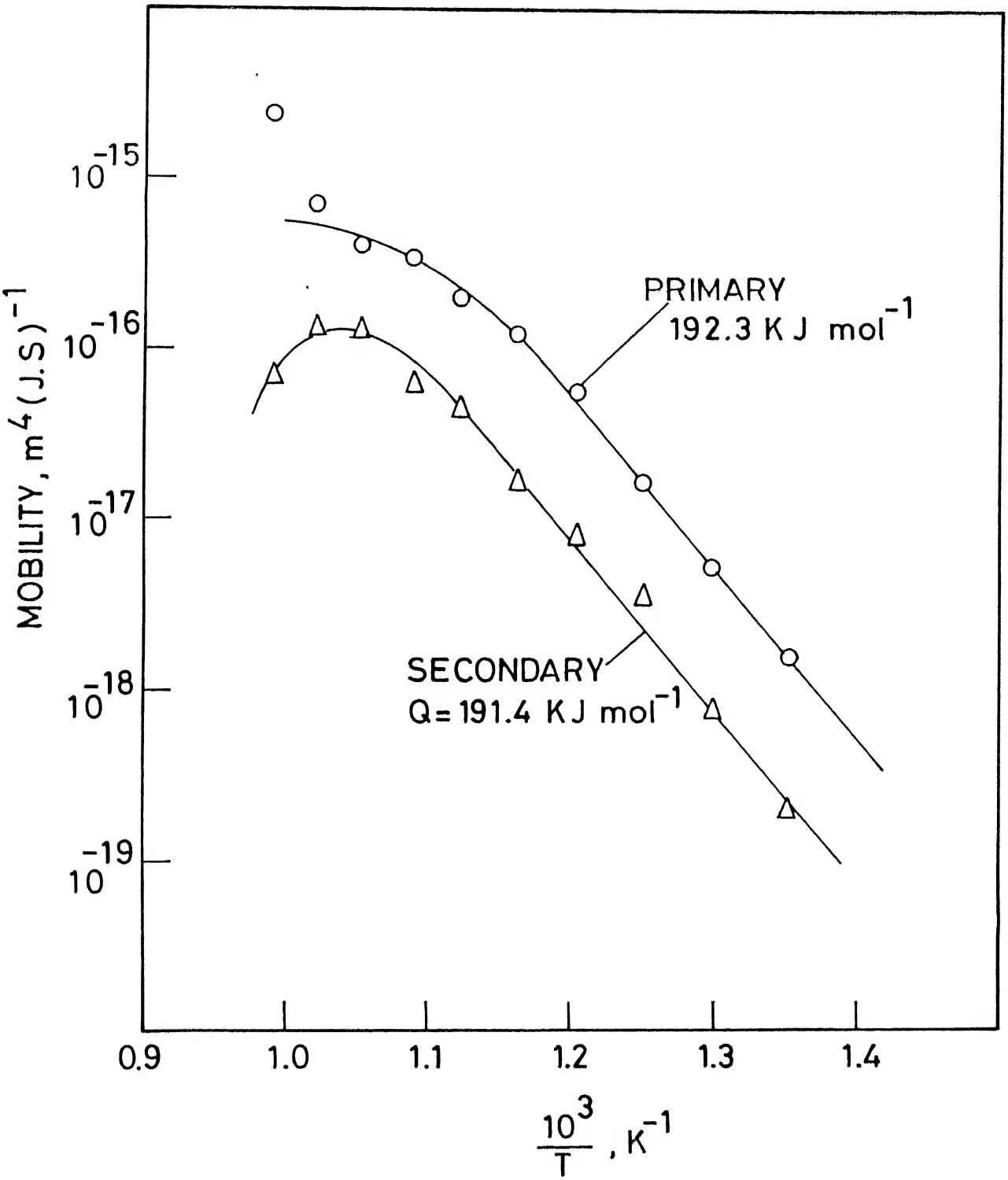

Fig. 3.9 Mobility Vs Temperature.

Table 3.5 : Mobility Vs Temperature values for Ni-4%In alloy

Temp (K)	Mobility (Primary) $M^4J^{-1}s^{-1}$	Mobility (Secondary) $M^4J^{-1}s^{-1}$
740	1.55×10^{-18}	2×10^{-19}
770	5.09×10^{-18}	8.12×10^{-19}
800	1.63×10^{-17}	3.64×10^{-18}
830	5.39×10^{-17}	8.1×10^{-18}
860	1.24×10^{-16}	1.65×10^{-18}
890	1.96×10^{-16}	4.40×10^{-17}
920	3.3×10^{-16}	6.28×10^{-17}
950	4.08×10^{-16}	1.30×10^{-16}
980	6.7×10^{-16}	1.33×10^{-16}
1010	2.42×10^{-15}	6.844×10^{-17}

Chapter 4. CONCLUSIONS

1. In Nickel alloys containing 4 at % In, discontinuous precipitation occurs in the temperature range 740 - 1010 K resulting in lamellar aggregate structure of α and θ. The transformation is controlled by the transport of solute through the advancing grain boundaries. The phenomenon of discontinuous coarsening is also controlled by transport of solute through the boundary

2. The growth rate of primary cells is higher by about two orders of magnitude of that of secondary cells and both of them show typical 'C' curve behaviour.

3. The interlamellar spacing of the primary and secondary cells increase with temperature. The interlamellar spacing of secondary cells are 2 - 4 times higher than that of primary cells.

4. The composition of the depleted matrix approaches equilibrium value after the secondary reaction whereas it is higher at the end of the primary reaction.

5. It can also be concluded from the calculation of activation energy considering the grain boundary mobility that the transport of solute through the boundary controls both the primary and secondary transformation.

6. The cell boundary diffusivities are seven to eight orders of magnitude higher than volume diffusivity of In in Ni but are of the same order of magnitude as the grain boundary diffusivity of In in Ni Thus the cellular precipitation and coarsening of the cellular precipitate with secondary cells can be regarded as processes requiring solute transport along the migrating grain boundaries.

References

[1] W. Graf : Diploma Thesis, Munster/Westf, 1-116, (1976)

[2] W. Gust, U Lenninger and B Predel · in proc. conf solid state phase transformation (ed. H. I Aarnson et al.) warrendale, pa, The Metall Soc AIME, 927 - 931, (1982)

[3] T. H. Chuang . D Sc., Thesis Stuttgart, 1 - 232, (1983)

[4] T. H Chuang, R.A.Fournelle, W. Gust and B. Predel · Acta Metall , 35, (1984)

[5] M. Fredel, G Duddek, M N. Faridani and B. Otte · Ber Bunsengers, Phys. Chem., 259 - 265, 82, (1978)

[6] S. Abdou, M. El- Boragy, W. Gust and B. Predel : paper presented at the conf of Solid State Phase Transformation, Cambrige, England, (1987)

[7] T. H. Chuang, R.A.Fournelle, W. Gust and B. Predel : Acta Metall , , (1987)

[8] R. Nakkalil and S. P. Gupta : Acta Metall , accepted for publication

[9] J. W. Cahn : Acta Metall., 7, 18, (1959)

[10] D. Turnbull : Acta Metall., 3, 55, (1955)

[11] M. Hillert : Acta Metall., 30, 1689, (1982)

[12] B. E. Sundquist : Metall. Trans , 4, 1919, (1973)

[13] J. Petermann and E. Hornbogen : Z. Metallk., 59, 814, (1975)

[14] H. Bohm : Z. Metallk., 52, 564, (1976)

[15] G. Meyrick · Scripta Met., 10, 649, (1976)

[16] C. S Smith : Trans. ASM., 45, 369, (1967)

[17] K. N. Tu and D Turnbull · Acta Metall., 15, 369, (1967)

[18] R. A. Fournelle and J. B. Clark : Met. Trans., 3, 2757, (1973)

[19] R. A. Fournelle : Acta Metall., 27, 1135, (1979)

[20] J. D Livingston and J. W. Cahn · Acta Metall , 22, 495, (1974)

E. Hellner . 'The Ni - In system' , Z. Metallk, 41, 401 - 406, (1950)

[22] E. A. Peretti . "Constitution of Indium alloy system", The Indium Corporation of America, (1959)

[23] M. F Singleton and P Nash " Bulletin of Alloy Phase Diagrams", 9, no 5, 592, (1988)

[24] N Gust, M. B Hintz, R Luic and B Preidel Met Res Soc Symp. Proc., 21, 513, (1983)

[25] M. Hansen and K. Anderko . Constitution of binary Alloys(McGraw - Hill, New York, (1958)

[26] T. B. Massalski : Binary Phase Diagrams Am Soc Metals, Metals Park, Ohio (1986)

[27] R. Hultgren, P. D Desai, D. T. Hawkins, M. Gleiser and K. K. Kelly . Selected Values of the Thermodynamic Properties of Binary Alloys, Am Soc Metals, Metals Park, Ohio (1973)

[28] W. Gust, M. B. Hintz, A. Lodding and H. Odelius · Phil - Mag, A 43, 1205 (1981)

[29] E D. Hondros and M. P. Seals : Interfacid and Surface Microscopy, Physical Metallurgy (edited by R W Cahn and P. Hassen), North Holland, Amsterdam (1983)

[30] S P. Gupta . Acta Metall., 35, 747 (1987)

[31] E. Nes and H. Billad · Acta. Metall., 25, 1039, (1977)

[32] C. Zener : Trans. AIME., 167, 500, (1946)